University of Kentucky
UKnowledge

University of Kentucky Master's Theses   Graduate School

2005

NONLINEAR TRANSIENT FINITE ELEMENT SIMULATIONS OF BEAM PARAMETRIC RESPONSE INCLUDING QUADRATIC DAMPING

Satish N.R. Remala
University of Kentucky

Right click to open a feedback form in a new tab to let us know how this document benefits you.

Recommended Citation

ABSTRACT OF THESIS

NONLINEAR TRANSIENT FINITE ELEMENT SIMULATIONS OF BEAM
PARAMETRIC RESPONSE INCLUDING QUADRATIC DAMPING

Nonlinear parametric response of a flexible cantilever beam is simulated. In the simulations, lateral response of the beam due to an imposed axial harmonic base displacement excitation is calculated. The response frequency is approximately half the input frequency. The transient simulations include the assumption of damping proportional to the square of the velocity along the beam. "Velocity-squared" damping is realistic for situations in which fluid forces resisting the structural motion are significant. The commercial finite element software, ANSYS, is used to perform the simulations. A flexible method is developed and implemented in this work, based on the ANSYS Parametric Design Language, for including the quadratic damping assumption in the analysis. Variation of steady state response amplitude is examined for a range of quadratic damping coefficients over a range of axial base excitation frequencies. Further, a definition of phase angle of the response with the respect to the input is proposed for these nonlinear cases in which the input frequency is an integer multiple of the response frequency. The response phase with respect to excitation is studied over a range of damping coefficients and excitation frequencies. In addition, numerical solutions of nonlinear dynamic systems obtained from the implicit finite element method and the explicit dynamics finite element method are compared. The nonlinear dynamic systems considered are a flexible beam subjected to axial base excitation and also lateral excitations. The studies comparing explicit and implicit method results include cases of stress-stiffening and large deflections.

KEYWORDS: Nonlinear, Parametric, Beam, velocity-squared damping, Finite elements.

Satish N.R. Remala

January 21, 2005

NONLINEAR TRANSIENT FINITE ELEMENT SIMULATIONS OF BEAM
PARAMETRIC RESPONSE INCLUDING QUADRATIC DAMPING

By

Satish N.R. Remala

Dr. John R. Baker
_____
Director of Thesis

Dr. George Huang
_____
Director of Graduate Studies

_____

RULES FOR THE USE OF THESIS

THESIS

Satish N.R. Remala

The Graduate School

University of Kentucky

2005

NONLINEAR TRANSIENT FINITE ELEMENT SIMULATIONS OF BEAM
PARAMETRIC RESPONSE INCLUDING QUADRATIC DAMPING

THESIS

A thesis submitted in partial fulfillment of the

Requirements for the degree of Master of Science in Mechanical Engineering in the

College of Engineering at the University of Kentucky

By

Satish N.R. Remala

Lexington, Kentucky

Director: Dr. John R. Baker, Assistant Professor of Mechanical Engineering

Lexington, Kentucky

2005

MASTER'S THESIS RELEASE

I authorize the University of Kentucky
 Libraries to reproduce this thesis in
whole or in part for the purpose of research.

 Signed: Satish N.R Remala
 Date: January 21, 2005

ACKNOWLEDGEMENTS

I would like to sincerely and wholeheartedly thank, my thesis director, Dr. John R. Baker for his guidance throughout this work. He has always been extraordinarily patient in answering tiniest and silliest details of my problems. I am extremely grateful to Dr John Baker for recommending to teaching assistantship. I would like to thank Dr. Suzanne Smith and Dr. Keith Rouch for being part of my thesis board despite their busy schedule.

Most importantly, I would like to thank my parents, Durga Prasad Rao and Indira Remala, and my sister, Sridevi, for their unconditional support and affection. Especially the encouragement from my sister, Sridevi, made everything easier to achieve. I am extremely thankful for her encouragement and affection.

TABLE OF CONTENTS

LIST OF TABLES

LIST OF FIGURES

LIST OF FILES

CHAPTER 1

INTRODUCTION

1.1 Motivation

Predicting nonlinear response of flexible structures is important in many fields. Engineers often first consider linear models to approximate response of the structures. But, as the flexibility of a structure increases, linear approximations often do not accurately predict the behavior. Hence nonlinear models are often necessary for predicting behavior of the flexible structures.

Some responses of nonlinearities associated with highly flexible structures are multiple resonances and jump phenomena. Flexible structures might experience resonance at an excitation frequency other than predicted linear natural frequencies, which is a combination of the linear natural frequencies and this phenomenon is known as multiple resonances. Bifurcation in nonlinear systems is a qualitative change in system behavior due to small variations of parameters of the system [3]. Parametric excitation is a very important nonlinear phenomenon considered for highly flexible structures, such as cables used for cable-stayed bridges and solar arrays of the international space station.

A beam is one of the basic elements of many structures. Beams are used in a wide variety of structural applications. Structures such as flexible solar arrays, long-span bridges, aircraft wings, and the rotor blades of a helicopter can be modeled as beam-like slender

members. Therefore, understanding nonlinear response of flexible beams for axial parametric excitation would be helpful in predicting response of more complex structures.

Finite element analysis (FEA) is a very popular method for numerical simulation in both research and industry. With the advent of high speed computer processors and storage capacity, different numerical integration algorithms are implemented in finite element codes to solve dynamic problems. Among various numerical integration methods developed over the past few decades were the central difference method, Newmark's numerical integration method, and Wilson method. These numerical methods are commonly referred to as either implicit methods or explicit methods. Every numerical integration algorithm has its own advantages and applicability for a particular application in terms of computational cost, stability and accuracy. The explicit method is useful for short transient problems, while the implicit method is useful for long transient problems. With the advances in the commercial finite element codes and numerical integration methods, now it is possible to predict geometrical nonlinearities and other nonlinear effects in structural behavior. An example of dynamic nonlinear structural behavior is lateral motion of a flexible beam in response to an axial excitation. This is typically a case of "parametric excitation", where the excitation frequency is different from the response frequency, and often the excitation frequency is an integer multiple of the response frequency.

Usually the lateral response of a flexible beam due to axial parametric excitation is damped by resistance of the surrounding air, and also by additional structural damping and increased stiffness due to large deflection. Air resistance limits the system lateral motion to some steady state amplitude. The force due to fluid resistance (drag) on any component of the system is determined by the Reynolds number for that component [25]. The drag force is proportional to velocity for low Reynolds numbers and the drag coefficient is inversely proportional to Reynolds number. For high Reynolds numbers, the drag force is proportional to the square of the velocity, and the drag coefficient is constant [3]. The drag coefficient is a function of the geometry and fluid properties [24]. Therefore, in this research, the transient response of a thin cantilever beam is simulated for axial excitation by applying quadratic damping using the capabilities of the commercial finite element code, ANSYS.

1.2 Scope of Thesis

The primary focus of this thesis is simulation of parametric response of a flexible cantilever beam assuming quadratic damping due to fluid forces. A contribution of this work is an overview of the use of ANSYS to study this phenomenon. Response of a flexible cantilever beam is simulated for cases of first mode excitation assuming a damping force proportional to the square of the velocity with a range of axial base excitation frequencies and a range of quadratic damping coefficients. Studies of phase difference between input and response are also performed for the transient responses for a range of excitation frequencies with quadratic damping. In addition, the implicit method

3

and explicit method are compared for transient response of linear and nonlinear dynamic systems.

1.3 Thesis Preview

This thesis has six chapters. Chapter 1 provides the motivation for this research and introduction to parametric vibrations. Chapter 2 describes structures exhibiting nonlinearities, analytical solutions and numerical solutions for these systems, and also provides a literature survey. Chapter 3 covers numerical methods implemented in commercial finite element codes, along with examples. Chapter 4 compares the implicit and explicit method solutions for linear and nonlinear dynamic systems. Chapter 5 presents nonlinear finite element transient simulations for cantilever beam response assuming velocity-squared damping for axial parametric excitation. Also, phase difference studies are performed where response phase with respect to input is considered. Finally, Chapter 6 summarizes this work and presents conclusions and suggestions for future work.

1.4 Introduction to Parametric vibrations

The nonlinear phenomena in which small parametric excitations can produce large response when the frequency of excitation is close to twice one of the natural frequencies of the system is know as principle parametric resonance[3]. Parametric resonance occurs in various structures. In forced vibration problems, energy is supplied into the system, and its response depends on various system parameters, including geometrical and material parameters [6]. Linear forced vibration problems do not lead to parameter

4

variation as a result of the imposed forcing function. But, in a nonlinear parametrically excited system, system parameters vary with time. In mathematical terms, the inhomogeneous differential equation of motion with constant coefficients for linear forced systems is replaced by a homogeneous differential equation with time-varying periodic coefficients [6].
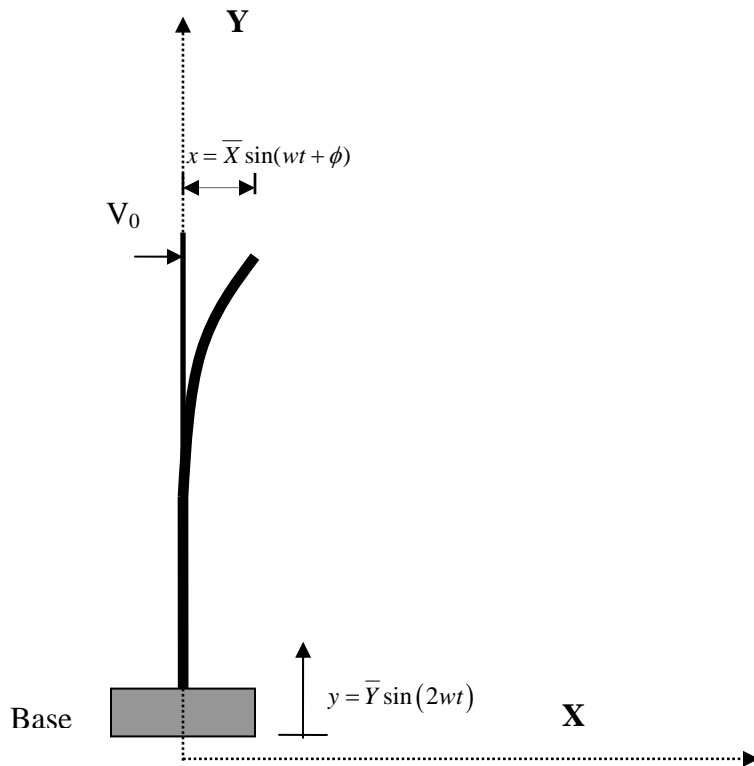
Figure 1.1: A thin Cantilever beam with axial base excitation

Figure 1.1 shows a schematic diagram of thin cantilever beam mounted on a mechanical shaker. For primary parametric resonance, the steady state motion of the beam, x(t), in the lateral direction (horizontal in the figure) is at a frequency near the beam's first mode natural frequency (ω)and the axial displacement input (y) is at frequency of near 2ω . Over the last few decades, much research was performed on nonlinear parametric response of a thin cantilever beam for axial harmonic excitation. Among the researchers, Crespo da Silva and Glynn[8,9], developed governing partial differential equations of

motion describing the nonlinear dynamics, where as Anderson T.J conducted analytical and experimental studies. Kuiyin Mei and Suzanne Smith simulated the transient response of the beam using the explicit solver of ANSYS/LS-DYNA [4, 5]. Chapter 2 provides a complete description of parametric vibration of an inverted cantilever beam.

CHAPTER 2

LITERATURE REVIEW

2.1 Structures Exhibiting Nonlinear Dynamic Response

Flexible structures can be found, for instance, in cable stayed bridges and space applications. Figure2.1 shows the cable stayed bridge (Fred Hartman Bridge) built at Houston, TX [27]. In long-span bridges, parametric vibration of large flexible cables might occur under the axial periodic load due to deck motion, or the bending vibration of the tower or wind loads [26]. Large space structures are the International Space Station and Hubble space telescope. Shown in Figure 2.2 is an artist's model of the International space station [28]. Components of the international space station, such as solar arrays and also components of space telescopes, such as radiators and membrane structures, are large and flexible. Because of their large size, combined with relatively low weight and stiffness, these components may exhibit nonlinear behavior. The nonlinear response of these components may affect the performance of the entire structure.

Figure 2.1: Cable Stayed Bridge (Fred Hartman Bridge at Houston, TX)

Photo: With the permission from Dr. Suzanne W. Smith

Figure 2.2: Artist's Concept of International Space Station

Photo Courtesy: NASA

Many researchers have performed beam studies to predict nonlinear behavior of components of large flexible structures. Over the last few decades, a lot of research has been carried out on nonlinear behavior of a cantilever beam with axial harmonic base excitation as shown in Figure 1.1. The following section gives a description of previous analytical and numerical studies performed on nonlinear behavior of thin cantilever beams. This thesis research builds on previous work on nonlinear beam analysis. Hence, previous beam studies are reviewed and presented in the following sections.

2.2 Analytical Solutions for Nonlinear Dynamic Response

In Nonlinear oscillations [3], Nayfeh and Mook provided examples of parametrically excited systems, and presented some analytical techniques for studying parametrically excited systems. Some of the analytical methods are Lindstedt-poincare technique, method of multiple scales, and Hill's method. Nayfeh and Mook [7] introduced perturbation techniques into analysis of nonlinear vibrations, which includes the method of multiple scales for the solutions of nonlinear oscillations and parametric vibrations. Anderson [5] provided a complete review on nonlinear analysis of beams. Anderson's PhD dissertation can be consulted for a thorough literature review.

Among the extensive studies on thin cantilever beams, Crespo Da Silva and Glynn [8, 9] developed a set of differential equations which includes nonlinearities due to inertia and curvature for three dimensional nonlinear flexural-flexural torsional motions of a long slender isotropic beam, and studied non planar, nonlinear forced oscillations for a fixed-free beam by applying perturbation techniques. They assumed bending and twisting

moments at any point along the beam are proportional to the nonlinear expressions of the local bending and twisting curvatures, and neglected warping, shear deformation and Poisson effects. Nayfeh and Pai [10] included third order shear deformation along with inertia and geometric nonlinearities in the analysis of parametric response of a thin cantilever beam. Anderson [5] theoretically and experimentally investigated effects of nonlinear curvature and damping in the response of a thin cantilever beam for parametric excitation. For theoretical studies, he considered equation (2.2.1) developed by Crespo Da Silva and Glynn [7, 8], and assumed linear viscous damping and quadratic damping for his analysis. The right hand side terms of the equation (2.2.1) correspond to nonlinear curvature, nonlinear inertia, axial base excitation, gravity and quadratic damping.

$$
m\frac{\partial^2 \hat{v}}{\partial \hat{t}^2} + \hat{\mu}\frac{\partial \hat{v}}{\partial \hat{t}} + EI\frac{\partial^4 \hat{v}}{\partial \hat{s}^4} = -EI\frac{\partial}{\partial \hat{s}}\left(\frac{\partial \hat{v}}{\partial \hat{s}}\frac{\partial}{\partial \hat{s}}\left(\frac{\partial \hat{v}}{\partial \hat{s}}\frac{\partial^2 \hat{v}}{\partial \hat{s}^2}\right)\right) - \frac{\partial}{\partial \hat{s}}\left(\frac{1}{2}\frac{\partial \hat{v}}{\partial \hat{s}}\int_L^{\hat{s}} m\frac{\partial^2}{\partial \hat{t}^2}\left(\int_0^{\hat{s}}\left(\frac{\partial \hat{v}}{\partial \hat{s}}\right)^2 ds\right)ds\right) -
$$

$$
m\left(\frac{\partial^2 \hat{v}}{\partial \hat{s}^2}(\hat{s}-L) + \frac{\partial \hat{v}}{\partial \hat{s}}\right)\left(\hat{a}_b\cos\left(\hat{\Omega}\hat{t}\right) + \hat{g}\right) - \hat{c}\frac{\partial \hat{v}}{\partial \hat{t}}\left|\frac{\partial \hat{v}}{\partial \hat{t}}\right|
$$

2.2.1

Where

m= Mass per unit length; $\hat{v}$ = Displacement; t=time;

$\hat{s}$ =Position along undeformed beam length; L=Length of undeformed beam

$\hat{\mu}$ =Coefficient of quadratic damping; I= Area moment of inertia;

$\hat{a}_b$ = Base acceleration of the beam along axis of the undeformed length

$\hat{\Omega}$ =Axial base excitation frequency

$\hat{c}$ = Quadratic damping Coefficient

Anderson [5] employed the method of multiple-scale to analyze solutions of nonlinear equations and focused on principle parametric resonance of the first two modes. The first four natural frequencies associated with his thin cantilever beam were 0.66 Hz, 5.69 Hz, 16.22Hz, and 32.06 Hz. Anderson [5] provided comparisons of theoretical and experimental frequency response and forced response results. Frequency response curves show variation in the beam's steady amplitude for a range of excitation frequencies. Anderson concluded that *inclusion of quadratic damping* in the analysis improved agreement between the theoretical and experimental frequency response results for the first mode. For the second mode, inclusion of quadratic damping did not improve agreement between theoretical and experimental results. He also concluded that for first mode excitation, the often neglected nonlinear curvature terms were stronger than nonlinear inertia terms, and lead to a nonlinear hardening effect. For the second mode of excitation, the nonlinear curvature effects dominate and lead to a nonlinear softening effect.

Arafat, et al. [12], investigated non planar, nonlinear response of inextensible cantilever beam subjected to axial base principle parametric excitation for two flexural modes. They assumed inextensionality condition and neglected torsional inertia in the derivation of integropartial differential equations of motions using Hamilton's extended principle from a Lagrangian and Virtual work, and applied the method of multiple scales to obtain modulation equations. Frequency response plots were generated using a pseudo arc length continuation scheme and stability was studied by calculating the Eigenvalues of

the Jacobian matrix. They presented detailed analysis for dynamic solutions of the modulation equations.

Hamdan, et al. [13], compared solutions obtained using the harmonic balance method and the method of multiple scales, and they also compared solutions from these methods with solutions obtained from numerical integration of equations of motion. Their studies involved parameter values corresponding to the first four modes of a flexible cantilever beam subjected to vertical harmonic base excitation. They concluded that the solution obtained from two term harmonic method gives accurate results for strong nonlinearities and multiple scales method breaks down at low amplitude for strong nonlinear cases.

Nayfeh, A.H, Yabuno, H. [14] investigated nonlinear normal modes of a flexible beam subjected to axial base parametric excitation by applying method of multiple scales and also by using a single mode Galerkin discretization. The nonlinear normal modes obtained from the multiple scale method were compared with results obtained from a single mode discretisation approach for different values of excitation frequencies. Their studies showed that nonlinear curvature and nonlinear damping were not influencing mode shapes obtained by a single discretization approach. As a result they concluded that a single-mode discretization approach might not give accurate mode shapes for the case of large amplitude oscillations.

2.3 Numerical Solutions for Nonlinear Dynamic Response

The finite element method is a numerical simulation method applied in a wide variety of engineering applications. Its use has expanded greatly with improvements in computing technology. Because of its versatility, it is indispensable for engineering simulations. Its applicability is accepted for both linear and nonlinear structural dynamic analysis. As mentioned in Chapter 1, the numerical integration methods used in transient finite element simulations are classified as explicit method or implicit method. This section presents reviews on explicit FEA analysis of flexible cantilever beams and comparisons of implicit and explicit methods for dynamic systems

Mei, K. [4, 16] simulated nonlinear transient response of a flexible cantilever beam. He studied axial base parametric excitation using the explicit dynamics finite element analysis approach. The Beam161 element of the commercial finite element software, ANSYS/LS-DYNA, was used for simulation of steady-state, large deformation transient response. He performed modal analysis and determined the first four natural frequencies (0.637 Hz, 5.61 Hz, 16.10 Hz and 31.76 Hz), which were in close agreement with Anderson's [5] experimental results. He assumed vertical sinusoidal base displacement excitation with amplitude appropriately scaled to match the base acceleration of Anderson experimental work. At the free end of the beam, a transverse velocity of 0.5 in/sec was applied as an initial condition. A range of excitation frequencies, near twice the first natural frequency were considered. He considered *damping directly proportional to velocity* in his analysis and applied modal damping as 0.32 percent of critical. Mei compared frequency response results obtained from his finite element results with

Anderson's experimental frequency response results. Mei concluded that his FEA results were consistent with Anderson's experimental results. Figure 2.3 compares FEA results with experimental results.
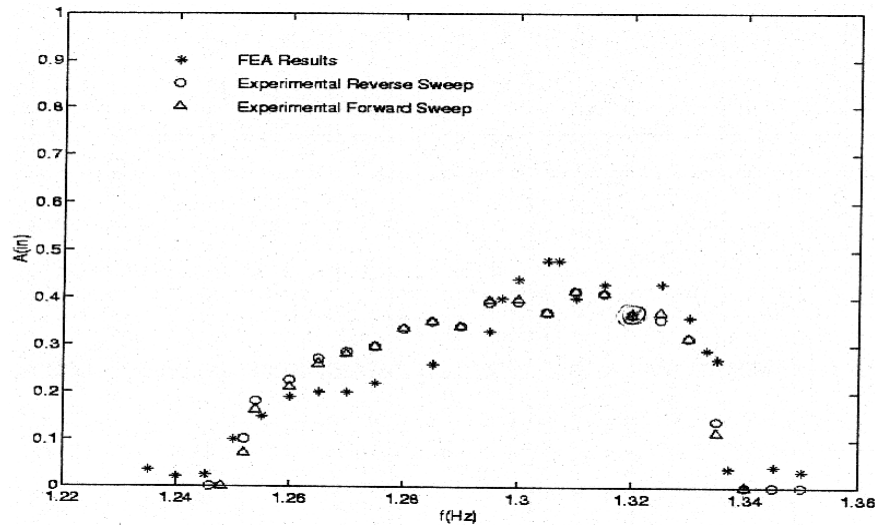
Figure 2.3: Comparison of Explicit Dynamics FEA results with experimental results [5]

Other researchers have compared implicit and explicit finite element analysis for different linear and nonlinear dynamic systems. Hu, et al. [17], compared explicit dynamic and implicit static finite element analysis results for sheet tensile tests and results showed that explicit method can be applied in simulation of quasistatic tensile tests only below critical test velocities. Rebelo, et al. [18], studied the effectiveness of implicit and explicit finite element analysis for static and dynamic metal forming problems using ABAQUS. Their studies showed that the implicit method is effective and faster than the explicit method for small wave front problems, but the explicit method is more effective than the implicit method for large complex problems. Sun, et al. [20], studied performance of implicit and explicit finite element methods for linear dynamic cases of (i) impact of elastic rod with rigid wall; (ii) impact of an elastic cylindrical disk

14

against a rigid wall; and (iii) slow contact between an elastic cylindrical disk and a rigid wall. The authors used ABAQUS for their comparisons. The results showed that the explicit method has advantages over the implicit method in terms of computational costs and accuracy for fast impact problems. For slow problems, the implicit method is better than the explicit method.

CHAPTER 3

NUMERICAL INTEGRATION METHODS

Finite element software employs numerical integration methods for the solution of linear equations. Among numerical integration methods, the Newmark time integration method and central difference method are implemented in many of the commercial finite element software packages. Also the Newton–Raphson method is a standard technique to update the stiffness matrix in nonlinear problems. The following sections give an overview of the Newmark method and central difference methods. The response of a simple example system is calculated using both the Newmark Method and Central Difference Method. It should be noted that the examples are provided to illustrate how the methods are implemented. The integration parameters, such as selected time step, in the examples in this chapter, are not necessarily optimized for solution accuracy or computational efficiency. The notations used in the following sections are consistent with Reference [1], Reference [22], and Reference [23].

3.1 Newmark Time Integration Method

As described in [1], the spatial discretisation of the structure leads to the governing equilibrium equation of structural dynamics, and can be expressed as

$$[M]\{\ddot{u}\} + [C]\{\dot{u}\} + [K]\{u\} = \{F^a\} \qquad (3.1.1)$$

16

$[M]$ = Mass matrix

$[C]$ = Damping Matrix

$[K]$ = Stiffness Matrix

$\{\ddot{u}\}$ = Acceleration vector

$\{\dot{u}\}$ = Velocity vector

$\{u\}$ = Displacement vector

$\{F^a\}$ = Applied load vector

The solution for this initial value problem is achieved numerically by discretising in time the continuous temporal derivatives that appear in Equation (3.1.1). Any one of the time integration procedures can be used for this purpose. The most widely used scheme among direct time integration methods for solving equation (3.1.1) is the Newmark time integration method.
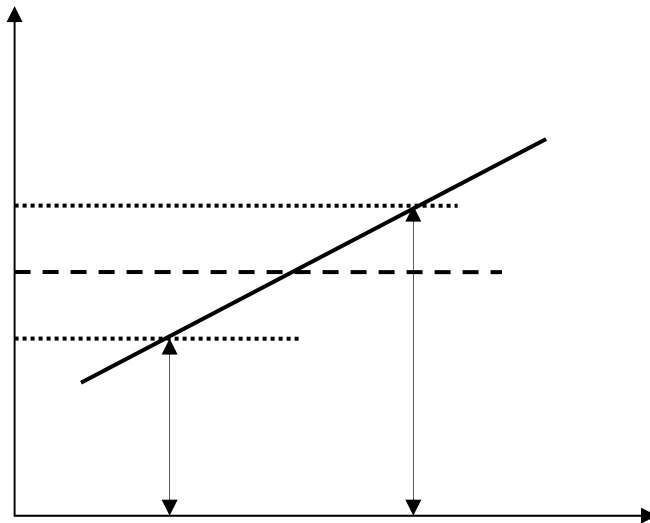
Figure 3.1: Constant Average Acceleration

17

The Newmark method utilizes finite difference expansion for the time interval Δt. As described in [1], Newmark time integration method uses following assumptions

$$\{\dot{u}_{n+1}\} = \{\dot{u}_n\} + [(1-\delta)\{\ddot{u}_n\} + \delta\{\ddot{u}_{n+1}\}]\Delta t \tag{3.1.2}$$

$$\{u_{n+1}\} = \{u_n\} + \{\dot{u}_n\}\Delta t + [(\tfrac{1}{2} - \alpha)\{\ddot{u}_n\} + \alpha\{\ddot{u}_{n+1}\}]\Delta t^2 \tag{3.1.3}$$

Where

α, δ = Numerical Integration parameters

$\Delta t = t_{n+1} - t_n$

$\{u_n\}$ =Displacement vector at time t_n

$\{\dot{u}_n\}$ =Velocity vector at time t_n

$\{\dot{u}_n\}$ =Velocity vector at time t_n

$\{\ddot{u}_n\}$ =Acceleration vector at time t_n

$\{u_{n+1}\}$ =Displacement vector at time $t_n + \Delta t$

$\{\dot{u}_{n+1}\}$ =Velocity vector at time $t_n + \Delta t$

$\{\ddot{u}_{n+1}\}$ =Acceleration vector at time $t_n + \Delta t$

$$[M]\{\ddot{u}_{n+1}\} + [C]\{\dot{u}_{n+1}\} + [K]\{u_{n+1}\} = \{F^a\} \tag{3.1.4}$$

Equilibrium equation (3.1.4) at $t_n + \Delta t$ is used along with equations (3.1.2) and (3.1.3) for the solution of the displacements, velocities, and accelerations. The solution for the displacement at time $t_n + \Delta t$ is obtained by deducing the equations (3.1.5) and (3.1.6) from equations (3.1.2) and (3.1.3)

$$\{\ddot{u}_{n+1}\} = a_0(\{u_{n+1}\} - \{u_n\}) - a_2\{\dot{u}_n\} - a_3\{\ddot{u}_n\} \tag{3.1.5}$$

$$\{\dot{u}_{n+1}\} = \{\dot{u}_n\} + a_6\{\ddot{u}_n\} + a_7\{a_0(\{u_{n+1}\} - \{u_n\}) - a_2\{\dot{u}_n\} - a_3\{\ddot{u}_n\}\} \tag{3.1.6}$$

Where

$$a_0 = \frac{1}{\alpha\Delta t^2} \quad a_1 = \frac{\delta}{\alpha\Delta t} \quad a_3 = \frac{1}{2\alpha} - 1 \quad a_4 = \frac{\delta}{\alpha} - 1 \quad a_5 = \frac{\Delta t}{2}\left(\frac{\delta}{\alpha} - 2\right) \quad a_6 = \Delta t(1-\alpha)$$

$$a_7 = \delta\Delta t$$

Substituting equations (3.1.5) and (3.1.6) in equation (3.1.4) results in the following equation.

$$(a_0[M] + a_1[C] + [K])\{u_{n+1}\} = \{F^a\} + [M](a_0\{u_n\} + a_2\{\dot{u}_n\} + a_3\{\ddot{u}_n\}) + [C](a_1\{u_n\} + a_4\{\dot{u}_n\} + a_5\{\ddot{u}_n\})$$
$$\tag{3.1.7}$$

From the above equation, the unknown quantity $\{\ddot{u}_{n+1}\}$ is calculated, and velocities and accelerations are updated by using equations (3.1.5) and equation (3.1.6).

In structural mechanics, a problem is nonlinear if the stiffness matrix or the load vector depends on the displacements. As discussed in [23], matrix $(a_0[M] + a_1[C] + [K])\{u_{n+1}\}$ in equation (3.1.7) is generally referred to as the effective stiffness matrix $[K]^{eff}$.

$$[K]^{eff} = (a_0[M] + a_1[C] + [K]) \tag{3.1.8}$$

For linear cases, the effective stiffness matrix remains constant in all the computational steps unless the time step is changed. For a nonlinear analysis, the effective stiffness changes at every time step and is displacement dependent.

For a nonlinear analysis, the effective stiffness matrix can be written as

19

$$[K]^{eff} = (a_0[M] + a_1[C_T] + [K_T])$$
$$(3.1.9)$$

Where

K_T = Tangential stiffness matrix

An iteration scheme such as Newton-Raphson, modified Newton-Raphson, or Quasi Newton methods can be employed to resolve the nonlinearity. The parameters, α and δ, determine the stability and accuracy characteristics of Newmark's method. As described in [30], the solution for equation (3.1.4) by means of Newmark equation (3.1.2) and equation (3.1.3) is unconditionally stable for

$$\alpha \geq \frac{1}{4}\left(\frac{1}{2} + \delta\right)^2, \ \delta \geq \frac{1}{2}, \ \frac{1}{2} + \delta + \alpha > 0$$

When $\delta = \frac{1}{2}$ and $\alpha = \frac{1}{4}$, equation (3.1.2) and equation (3.1.3) correspond to constant average acceleration method [22]. The method is implicit, unconditionally stable, second-order accurate, and one of the most effective and popular methods for structural dynamics problems.

3.1.1 Simple Example

For a simple example, this section will show the solution for the unit step response of the single degree of freedom system shown in figure (3.2) using the Newmark time integration method. The values for mass, damping, and stiffness are $M = 2kg$, $B=4$ $N\text{-}s/m$ and $K=18$ N/m. The input is a unit step function, so $F=1$ for $t > 0$. The initial conditions for displacement, u, and velocity, $\dot{u}$, are $u(0) = 0$ and $\dot{u}(0) = 0$
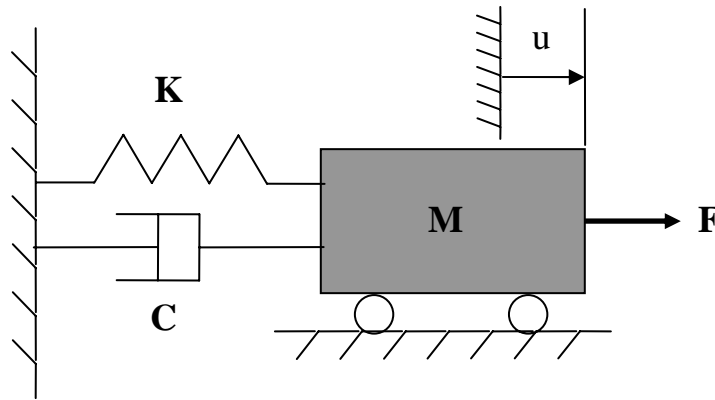
Figure3.2: Single Degree of freedom system with unit step input

The Newmark integration parameters assumed for this case are $\alpha = 0.25$ and $\delta = 0.5$.The time step is selected as $\Delta t = 0.1$. The displacement, velocity, and acceleration for each time step are calculated using a MATLAB m-file. Seventy iterations are performed to get the steady state solution. The table 3.1 shows the values of displacement, velocity and acceleration for first 2.0 seconds. This table also shows the exact solution for displacement for this case. Figure3.3 shows displacement response for a unit step input as a function of time. The MATALAB m-file written to implement the numerical integration is shown in Appendix A

Table 3.1: Values for displacement, velocity and acceleration by Newmark method

Time(t) (sec)	Displacement $u(t)$	Exact Solution for $u(t)$	Velocity $\dot{u}(t)$	Acceleration $\ddot{u}(t)$
0 .0000	0.0000	0.0000	0 .0000	0 .0000
0.1000	0.0011	0.0023	0.0223	0.4454
0.2000	0.0053	0.0085	0.0611	0.3304
0.3000	0.0127	0.0174	0.0880	0.2093
0.4000	0.0223	0.0278	0.1032	0.0930
0.5000	0.0328	0.0385	0.1073	-0.0100
0.6000	0.0433	0.0487	0.1021	-0.0939
0.7000	0.0529	0.0576	0.0897	-0.1552
0.8000	0.0610	0.0647	0.0722	-0.1933
0.9000	0.0672	0.0698	0.0521	-0.2090
1.0000	0.0714	0.0728	0.0314	-0.2052
1.1000	0.0735	0.0738	0.0119	-0.1856
1.2000	0.0739	0.0732	-0.0051	-0.1546

Table 3.1 Continued:

1.3000	0.0727	0.0713	-0.0187	-0.1167
1.4000	0.0703	0.0685	-0.0283	-0.0763
1.5000	0.0672	0.0651	-0.0340	-0.0369
1.6000	0.0637	0.0615	-0.0359	-0.0016
1.7000	0.0602	0.0582	-0.0346	0.0276
1.8000	0.0569	0.0552	-0.0308	0.0493
1.9000	0.0541	0.0528	-0.0252	0.0632
2.0000	0.0519	0.0510	-0.0185	0.0696
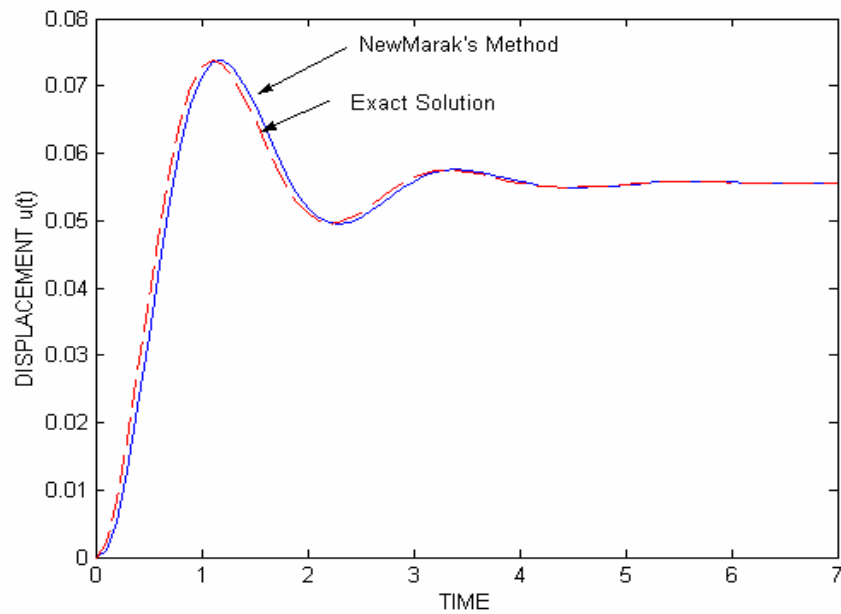
Figure 3.3: comparison of Newmark's method with exact solution for single degree of

freedom system for unit step input

3.2 Central Difference method

The central difference method can be used in what is commonly referred to an "explicit" method. The central difference method is based on finite difference expressions in time for velocity and acceleration.
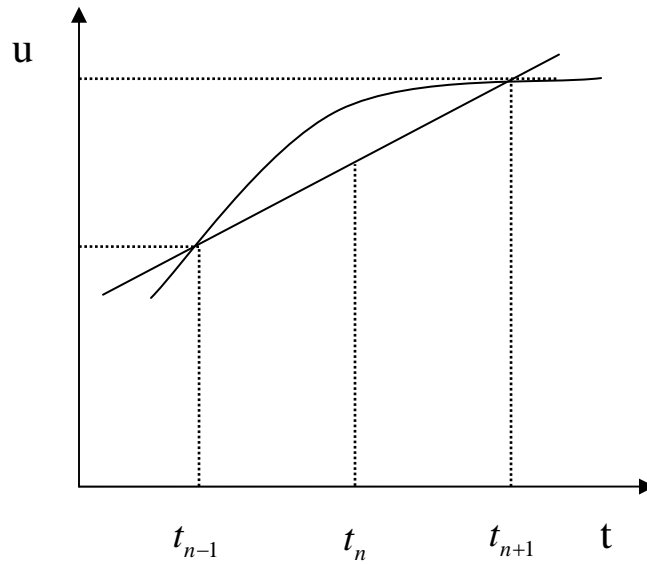
Figure 3.4: Linear displacement change

As given in Bathe [22], the central difference method uses following assumptions

$$\{\dot{u}_n\} = \frac{\{u_{n+1}\} - \{u_{n-1}\}}{2\Delta t} \tag{3.2.1}$$

$$\{\ddot{u}_n\} = \frac{1}{\Delta t^2}(\{u_{n+1}\} - 2\{u_n\} + \{u_{n-1}\}) \tag{3.2.2}$$

$\{u_n\}$ =Displacement vector at time t_n

$\{\dot{u}_n\}$ =Velocity vector at time t_n

$\{\ddot{u}_n\}$ =Acceleration vector at time t_n

$\{u_{n+1}\}$ = Displacement vector at time $t_n + \Delta t$

$\{\dot{u}_{n+1}\}$ = Velocity vector at time $t_n + \Delta t$

$\{\ddot{u}_{n+1}\}$ = Acceleration vector at time $t_n + \Delta t$

$\{u_{n-1}\}$ = Displacement vector at time $t_n - \Delta t$

$\{\dot{u}_{n-1}\}$ = Velocity vector at time $t_n - \Delta t$

Equations (3.2.1) and equation (3.2.2) are obtained by expanding $\{u_{n+1}\}$ and $\{u_{n-1}\}$ in a

Taylor series about time $n\Delta t$

$$\{u_{n+1}\} = \{u_n\} + \Delta t\{\dot{u}_n\} + \frac{\Delta t^2}{2}\{\ddot{u}_n\} + \frac{\Delta t^3}{6}\{\dddot{u}_n\} + \cdots\cdots\cdots \qquad (3.2.3)$$

$$\{u_{n-1}\} = \{u_n\} - \Delta t\{\dot{u}_n\} + \frac{\Delta t^2}{2}\{\ddot{u}_n\} - \frac{\Delta t^3}{6}\{\dddot{u}_n\} + \cdots\cdots\cdots \qquad (3.2.4)$$

Equation (3.2.1) is obtained by subtracting equation (3.2.4) from equation (3.2.3), while

adding equation (3.2.4) and equation (3.2.3) yields equation (3.2.2). In both cases, terms

containing Δt^2 and higher powers are omitted from equation (3.2.1) and equation (3.2.2).

So, the error in the expansion is of the order Δt^2. The displacement solution for time $t_n +$

Δt is obtained by considering equation (3.1.1) at time t

$$[M]\{\ddot{u}_n\} + [C]\{\dot{u}_n\} + [K]\{u_n\} = \{F^a\} \qquad (3.2.5)$$

Substituting the relations for $\{\ddot{u}_n\}$ and $\{\dot{u}_n\}$ in (3.2.1) and (3.2.2), respectively into

(3.2.5), we obtain

$$\left(\frac{1}{\Delta t^2}[M] + \frac{1}{2\Delta t}[C]\right)\{u_{n+1}\} = \{F^a\} - \left([K] - \frac{2}{\Delta t^2}[M]\right)\{u_n\} - \left(\frac{1}{\Delta t^2}[M] - \frac{1}{2\Delta t}[C]\right)\{u_{n-1}\}$$

$$(3.2.6)$$

In general, the smaller the value of the Δt, the more accurate the solution, but the number of computations will then increase. There are errors with each iteration due to the truncation of the Taylor series. Central difference integration methods do not require a factorization of the effective stiffness matrix in the step by step solution. The effectiveness of the central difference method depends on efficient performance of the each time step solution. Because of the small step size, a large number of time steps usually are needed. Therefore, the method is typically applied only when a lumped mass matrix is considered. Considering a case with no damping, Equation (3.2.6) reduces to

$$\left(\frac{1}{\Delta t^2}[M]\right)u_{n+1} = F^{eff} \tag{3.2.7}$$

Where

$$F^{eff} = F^a - \left([K] - \frac{2}{\Delta t^2}[M]\right)\{u_n\} - \left(\frac{1}{\Delta t^2}[M]\right)\{u_{n-1}\}$$

If the mass matrix is diagonal, the system of equations in (3.1.1) can be solved without factorization of a matrix. Only matrix multiplications are required to obtain the right hand side effective load vector, after which the displacement components are obtained using

$$u_{n+1} = F^{eff}\left(\frac{\Delta t^2}{[M]}\right) \tag{3.2.8}$$

The advantage of using the central difference method in the form (3.2.8) is no stiffness matrix of complete assemblage needs to be calculated. As described in [22], by the central difference method, the solution is essentially carried out on the element level and relatively high speed storage is required. Using the central difference method, a system of very large order can be solved effectively.

3.2.1 Simple example

For a simple example, this section will show the solution for the unit step response of the same system of section 3.1.2 shown in figure (3.2) using central difference method. The values of mass, damping, and stiffness are *M=2kg*, *B=4 N-s/m* and *K=18 N/m* and *F=1*. The time step taken for calculation of the solution is 0.1 seconds. Displacement, velocity, and acceleration for each time step are calculated using a MATLAB m-file((provided in Appendix B). Seventy iterations are performed to arrive at the steady state solution .The following table shows the values of displacement, velocity and acceleration for the first 2.0 seconds. Figure 3.5 compares response obtained from central difference method with exact solution for single degree of the freedom system as a function of time as calculated by central difference method.

Table3.2: Values for displacement, velocity and acceleration by central difference method

Time(t) (sec)	Exact solution for $u(t)$	Displacement $u(t)$	Velocity $\dot{u}(t)$	Acceleration $\ddot{u}(t)$
0.0000	0.0000	0.0000	0.0000	0.0000
0.1000	0.0023	0.0001	0.0024	0.0000
0.2000	0.0085	0.0051	0.0997	0.4945
0.3000	0.0174	0.0127	0.1012	0.2547
0.4000	0.0278	0.0221	0.1124	0.1836
0.5000	0.0385	0.0323	0.1094	0.0764
0.6000	0.0487	0.0423	0.0999	-0.0090
0.7000	0.0576	0.0516	0.0846	-0.0808
0.8000	0.0647	0.0595	0.0660	-0.1338

Table 3.2 Continued:

0.9000	0.0698	0.0658	0.0458	-0.1678
1.0000	0.0728	0.0702	0.0258	-0.1838
1.1000	0.0738	0.0728	0.0075	-0.1836
1.2000	0.0732	0.0737	-0.0082	-0.1702
1.3000	0.0713	0.0731	-0.0205	-0.1468
1.4000	0.0685	0.0713	-0.0292	-0.1168
1.5000	0.0651	0.0688	-0.0343	-0.0836
1.6000	0.0615	0.0657	-0.0360	-0.0502
1.7000	0.0582	0.0624	-0.0347	-0.0190
1.8000	0.0552	0.0592	-0.0312	0.0081
1.9000	0.0528	0.0563	-0.0261	0.0299
2.0000	0.0510	0.0538	-0.0199	0.0457
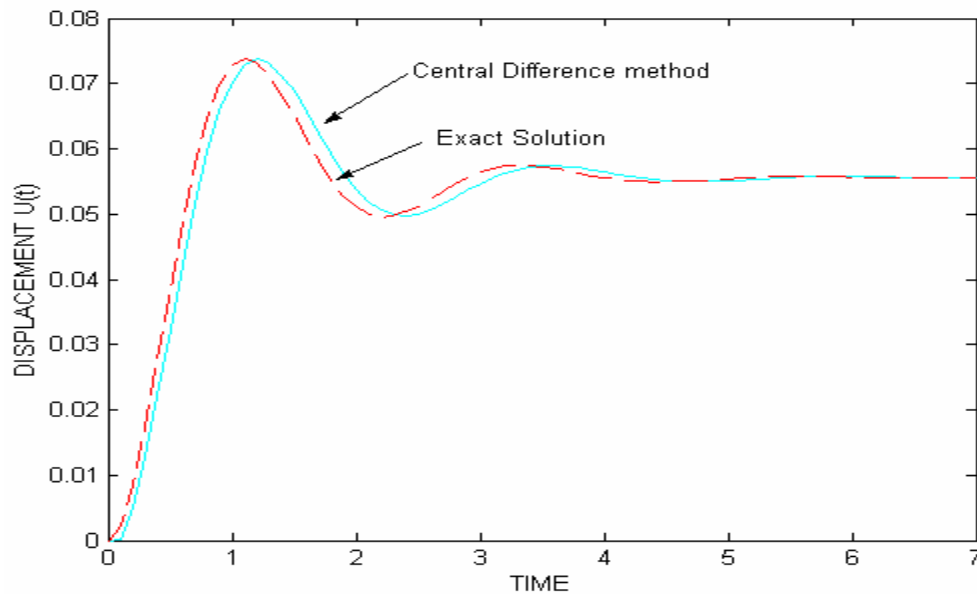
Figure 3. 5: comparison of central difference method with exact solution for single degree

of freedom system for unit step input

3.3 Newton-Raphson Method for Large Deflection Nonlinearities

The Newton-Raphson is a most widely used numerical approximation method to solve nonlinear problems. For large deflections, the effective stiffness matrix is function of deflection. Therefore, most commercial finite element software employs the Newton-Raphson method, along with implicit numerical integration methods to provide solution for nonlinear structural problems. Since this is a well-known method, the details will not be provided here. A complete description of Newton–Raphson method is available in References [22, 23]

CHAPTER 4

SIMULATION STUDIES ON BEAMS: IMPLICIT VS EXPLICIT

4.1 Implicit Method Vs Explicit Method

Numerical solution schemes are often classified as being implicit or explicit. As defined in Reference [21] "When a direct computation of the dependent variables can be made in terms of known quantities, the computation is said to be explicit. In contrast when the dependent variables are defined by coupled sets of equations, and either a matrix or iterative technique is needed to obtain the solution, the numerical method is said to be implicit". If lumped mass and lumped damping matrixes are used, the central difference method is an explicit method where as Newmark's integration method is an implicit time integration method. Most of the material presented in this section is adopted form references [1], [2], [21], and [22].

The commercial finite element software, ANSYS, uses Newmark's time integration method for the solution of transient problems, and for the nonlinear dynamics solutions, the Newton-Raphson method is employed along with Newmark's method. The implicit method uses Equation (4.1.1) to obtain the solution

$$\{u_{n+1}\} = [K]^{-1}\{F_{n+1}{}^{a}\} \tag{4.1.1}$$

In the implicit time integration method, the inverse of the stiffness matrix [K] is calculated for each increment of time step Δt to solve for displacement $\{u\}$. This

approach is a CPU intensive operation and it is computationally expensive. For the nonlinearities, [K] is also a function of displacement {u}, so [K] is obtained by series of linear approximations (Newton – Raphson) as well.

Some commercial finite element software like ANSYS/LS-DYNA, ABAQUS, and MSC Dytran also include the explicit time integration method (central difference time integration method). As given in reference [1], an explicit method uses the equation (4.1.2) to obtain the solution.

$$\{\ddot{u}_n\} = [M]^{-1}\left(\{F_n^{Ext}\} - \{F_n^{Int}\}\right) \tag{4.1.2}$$

Where

F_n^{Ext} = Applied external and body force

F_n^{Int} = Internal force vector

From reference [1]

$$F^{Int} = \sum(\int_\Omega B^T \sigma_n d\Omega + F^{hg}) + F^{contact} \tag{4.1.3}$$

Where

F^{hg} = Hour glass resistance force

$F^{contact}$ = Contact force

The explicit method calculates the inverse of the mass matrix [M] to solve for acceleration $\{\ddot{u}\}$, and assumes a lumped mass matrix [M]. Because the mass matrix [M] is lumped (diagonal terms only), inversion of the mass matrix [M] is not CPU – intensive. For the nonlinearities, the equation are uncoupled, and can be solved for directly

31

(explicitly) and the stiffness matrix [K] does not need to be inverted. All the nonlinearities (including contact) are included in the internal force vector. The major computational expense is in calculating internal forces, and CPU cost is approximately proportional to the size of the finite element model and does not change as dramatically as it does in the implicit method.

If the solution remains well behaved for arbitrarily large values of the time step, the method is said to be unconditionally stable. For linear problems, the implicit solution is unconditionally stable. For nonlinear problems, the time step may become small due to convergence difficulties. Though convergence checking is performed within the software, convergence is not guaranteed for highly nonlinear problems solved by the implicit method. For the explicit method, the very small steps are required to maintain stability. The stability limit for an explicit operator is that the maximum time increment must be less than a critical value of the smallest transition times for a dilatational wave to cross any element in the mesh.

$$\Delta t \leq \Delta t^{Critical} = \frac{2}{\omega_{max}}$$ (4.1.4)

ω_{max} = Largest natural frequency

Because of very small step size, the explicit method is useful for very short transient problems. Convergence checks are not need for explicit solutions because equations are uncoupled. The explicit method is ideally suited for wave propagation types of problems (structures subjected to impact and blast loads). For the beam and truss elements, the critical time step is calculated by equation (4.1.5)

$$\Delta t^{Critical} = \frac{L}{c} \tag{4.1.5}$$

$$c = \sqrt{\frac{E}{\rho}} \tag{4.1.6}$$

Where

C= Wave propagation velocity;

E= Young's Modulus;

ρ = Mass Density;

Therefore the implicit method and explicit method have their own applicability and advantages in terms of computational cost, accuracy and stability to a particular problem. Hence in Section 4.2, transient response of a cantilever beam subjected to a range of loading conditions were solved by using the commercial implicit finite element solver, ANSYS, and commercial explicit finite element solver, ANSYS/LS-DYNA. In Case 1, a lateral step input is applied to the beam. In Case 2, a lateral harmonic load is applied with no axial load. In Case 3, a lateral harmonic load is applied with a range of constant axial loads as a study on the effect of stress-stiffening. The solutions obtained from both the methods for these three example cases are compared for computational costs, stability and accuracy. Then, in Section 4.3, a fourth set of example cases is provided, in which both methods are applied to nonlinear transient response of a flexible cantilever beam subjected to axial parametric base excitation.

4.2 Beam Response Studies for Lateral Input / Lateral Response: Implicit and Explicit methods

A cantilever beam with various loading conditions was considered as a basis for comparison of explicit and implicit methods. The beam has a rectangular cross-section of 0.75×0.128 inches and a length of 33.56 inches. Material properties assumed for the beam are: Young's modulus (E) = 30×10^6 lb/in^2; Density (ρ) = 0.00073 lb.s^2/in^4; Possion's ratio (γ) =0.29. The first natural frequency obtained from a modal analysis was 3.880 Hz. For all the cases, The ANSYS 2D beam element, Beam3, was used for the implicit finite analysis, and the Beam161 element of ANSYS/LS-DYNA was used for the explicit finite analysis. The cantilever beam was modeled using 40 nodes, with 39 elements, for both implicit finite element and explicit finite element analysis. The ANSYS Beam3 element is 2-D elastic uniaxial beam with tension, compression and bending capabilities. It allows for stress stiffening and nonlinearities due to larger deflections. The 3-D beam element, Beam161 (Belytschko beam), employs standard co-rotational techniques for large deflection problems. In ANSYS/LS-DYNA, Key option (1) can be used to form the Belytschko beam. In ANSYS, proportional damping can be implemented by using a mass matrix multiplier (α) and/or a stiffness matrix multiplier (β). The effective damping ratio is linearly related to frequency for beta damping and consequently has a large effect on higher frequency content. For Alpha damping, the effective damping ratio is inversely related to frequency, so alpha damping has large effect on low frequencies. For these cases, mass proportional damping is assumed, so that a damping matrix is formed as the product of the mass matrix, and a mass matrix

34

multiplier, α. The mass matrix multiplier (α) can be calculated to produce a desired effective damping ratio, ζ, for motion at some frequency, ω, based on the relationship

$$\alpha = 2 \times \omega \times \zeta \qquad (4.2.1)$$

4.2.1 CASE 1: Transient Dynamic analysis with Unit Step Load

As a first comparison study, transient dynamic analysis was performed on a cantilever beam subjected to unit step load at its free end. Figure 4.1 shows a schematic diagram of the cantilever beam subjected to a unit step load.
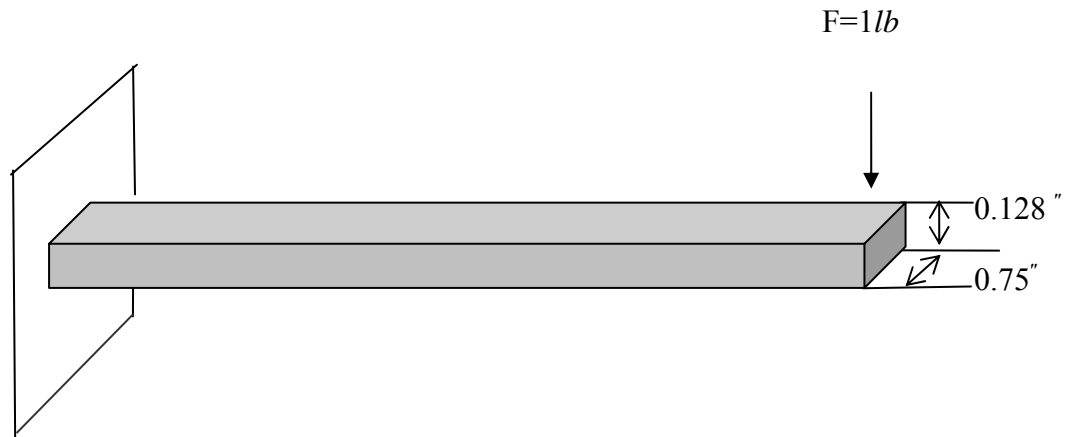
Figure 4.1: Schematic diagram of a cantilever beam with unit step load

The "full" method option for transient dynamic analysis was selected for the implicit analysis. ANSYS also has options allowing for transient analysis using a reduced model or based on subsets of modes. An initial time step of 0.1 sec was assumed for the implicit analysis. After the initial time step, ANSYS used automating time stepping. For the explicit analysis, the default scale factor of 0.9 for computing the time step was used. This factor is multiplied by the critical time step. The critical time step is a function of minimum element size and material properties. Geometric nonlinearities and stress

35

stiffening effects were included in the analysis. Gravity loading was also applied in the lateral direction of the beam, along with the step load. Figure 4.2(a) shows the response of the lateral free end of the cantilever beam obtained from the implicit finite element method and Figure 4.2(b) shows the lateral free end response obtained from the explicit dynamics finite element method.

(a)   (b)
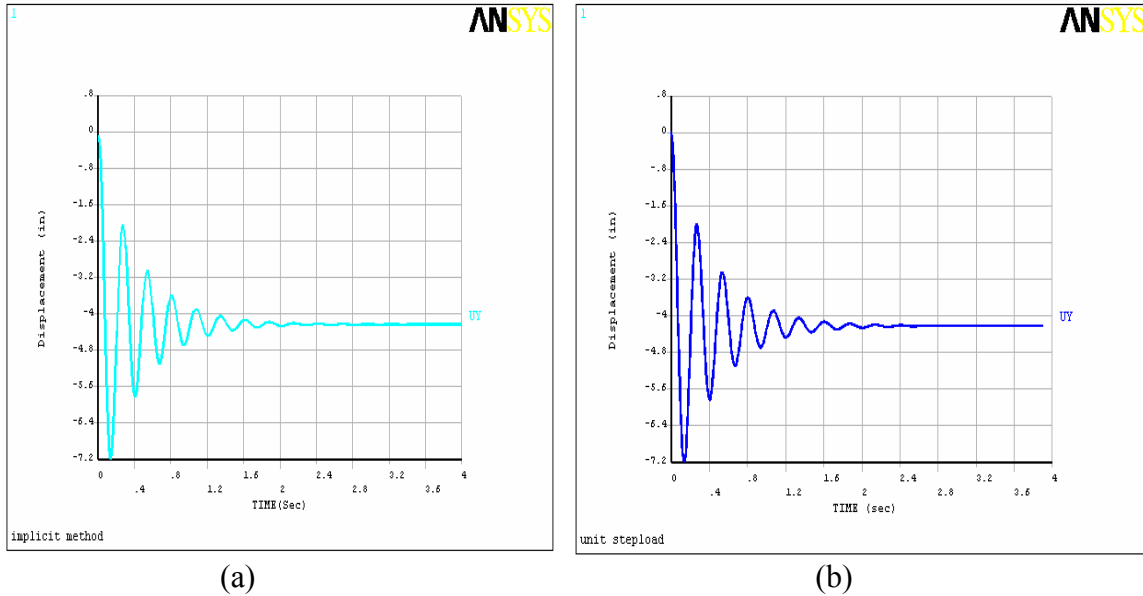
Figure4.2: Response at the free end of the beam for lateral unit loading obtained from a) implicit method b) explicit method.

A damping ratio of 0.1 was assumed for the first mode natural frequency, and the corresponding alpha damping value was calculated by using equation 4.2.1. On a computer (Pentium IV (2.8GHz) Main memory 512MB), the implicit method took 123 seconds of CPU time for solving, while the explicit method took 223 seconds of CPU time for the solution. Table (4.1) compares steady state values obtained with the implicit and explicit method. The steady state values are compared for the unit step load and gravity. Both the methods produced accurate results when compared with theoretical

36

results. As noted above, since automatic time stepping was used in the implicit analysis, the efficiency of the implicit analysis considered here was determined to a large extent by internal programming in ANSYS. The primary motivation for these examples was to gain some insight into how the results would compare for identical loading using the two different solution methods, and to make some observations on how the solution times would compare. Certainly, a more in-depth study could be undertaken in which a range of settings could be considered and compared, such as selected time step in the implicit analysis, and selected time step scale factor in the explicit analysis. The primary goal of this work was to determine a viable method for implementing quadratic damping in nonlinear studies of beam response, so an exhaustive study comparing efficiencies of the implicit and explicit methods was beyond the scope of this work.

Table (4.1): steady state values obtained with the implicit and explicit method for a step load

	Deflection (UY) Due force P=1lb At Free end(node40) inches	Deflection (UY) Due force GRAVITY At free end(node 40) inches
IMPLICIT	3.17472	1.09104
EXPLICIT	3.15000	1.08574
THEORETICAL	3.20414	1.10002

Table 4.2 compares maximum overshoot obtained from explicit and implicit analysis with different damping ratios for the first mode natural frequency. From the table, we can conclude that maximum over shoot obtained from both the methods were identical.

Table 4.2: Comparison of maximum over shoot values for unit step load

Damping ratio (Zeta)	Maximum Overshoot Implicit method	Maximum Overshoot Explicit method
0.1	7.18585	7.17109
0.075	7.42050	7.40238
0.05	7.67184	7.66114
0.025	7.94143	7.93340
0.01	8.11270	8.10640

4.2.2 CASE 2: Transient Dynamic analysis with Harmonic Load

Transient dynamic analysis was performed on a cantilever beam subjected to a harmonic load at its free end. Figure4.3 shows a schematic diagram of a cantilever beam subjected to harmonic excitation at its free end.

$$F = 1 \times \sin(w_1 t)$$

$0.128''$

$0.75''$
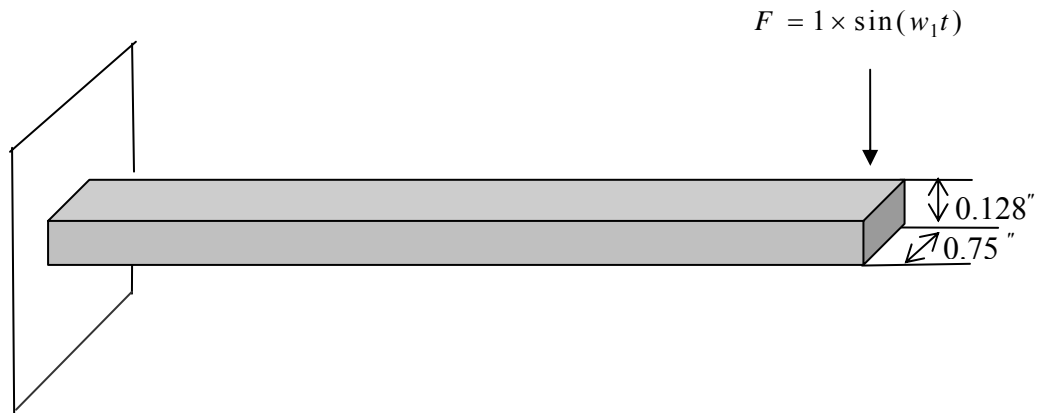
Figure 4.3: Schematic diagram for Cantilever beam subjected to harmonic load

The beam was excited with a frequency equal to half of its first natural frequency. So the excitation frequency was 1.860635 Hz. Alpha damping was applied, with mass matrix multiplier, α, equal to 0.46768. Geometric nonlinearities were included in the analysis. Gravity loading was applied in the direction lateral to the beam. Figure 4.4 shows response of the free end of the beam as a function of time for both the implicit and

explicit method for the first 40 seconds after the start of the application of the harmonic load.
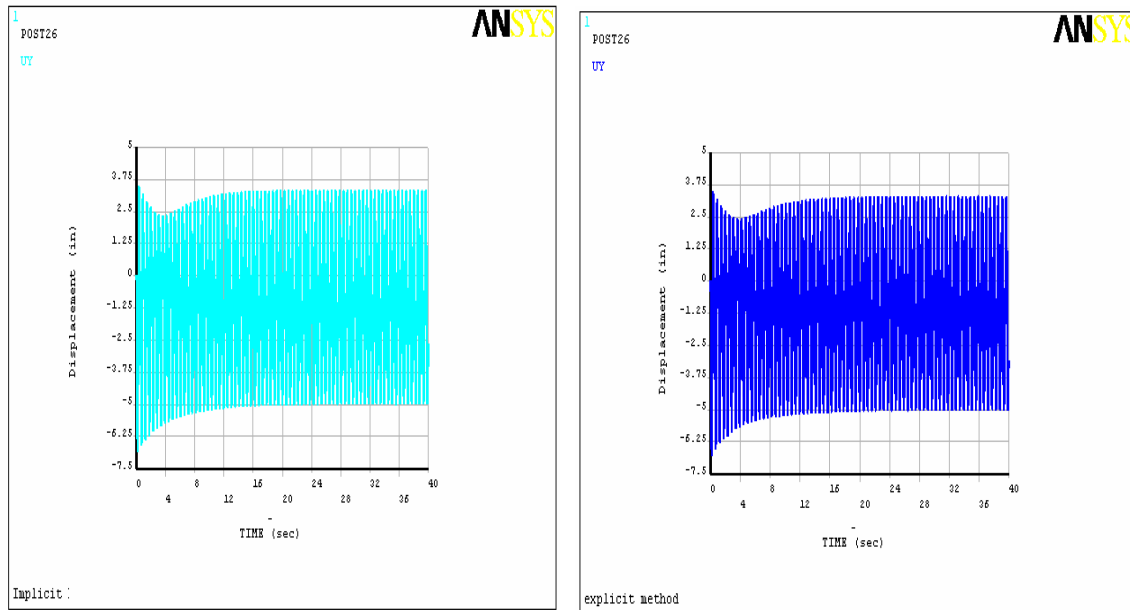
          (a)   (b)

Figure4.4: Amplitude response obtained from a) implicit method b) explicit method for lateral harmonic excitation

To avoid convergence problems, a small initial time step of 0.01 was selected for the implicit analysis, while for the explicit analysis, the default scale factor of 0.9 for the computed time step was used. In this case, as in Case 1, again, automatic time stepping was used in the implicit analysis. Apparently because a relatively small time step size was used in the implicit analysis, based on the preprogrammed automatic time stepping procedures, the implicit method took 9120 seconds (2 hours 32 minutes) of CPU time for solving on a computer (Pentium IV (2.8GHz) Main memory 512MB), while the explicit method took only 806 seconds of CPU time for solution. In this case, clearly the explicit method was significantly faster, and the results from both cases are very close to the same.

39

4.2.3 CASE 3: Transient Dynamic analysis with Stress Stiffening effects

As a third example, a transient dynamic analysis was performed on a cantilever beam subjected to a harmonic load in its lateral direction and step load in its axial direction simultaneously at its free end. This case was used to determine if the effect of stress stiffening would produce significant differences between the two numerical integration methods. In this case, three different values of step loads in the axial direction were considered for the same harmonic loading at the free end of the beam. Figure4.5 shows a schematic diagram of applying a harmonic load in the lateral direction and a step load in the axial direction at the free end of the cantilever beam.

$$F_L = 1 \times \sin(w_1 t)$$

$$F_A = 1lb$$
(Step load)
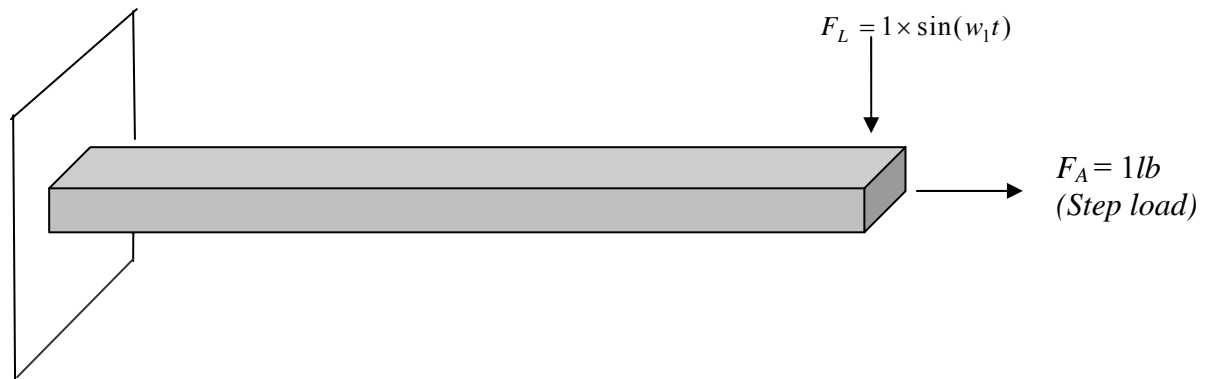
Figure 4.5: Schematic diagram for Cantilever beam subjected to harmonic excitation and step load (1 *lb*)

The beam is excited harmonically at its free end, with an excitation frequency of f_{ex}=1.860635Hz. The beam was subjected to a load of F_L= 1sin (w_1t) in the lateral direction, and a step load of 1*lb* in axial direction at free end. Alpha damping was applied with a mass matrix multiplier of 1.1692. Geometric nonlinearities were included in the analysis. Gravity loading was applied in the direction lateral to the beam. An initial time

step of 0.01 was selected for the implicit analysis, and automatic time stepping was used. For the explicit analysis, the default scale factor of 0.9 for the computed time step was selected. Figure(4.6) shows the lateral free end response obtained from the explicit finite method and implicit finite method for this case. The implicit method only took 280 seconds of CPU time for solving, while the explicit method took only 440 seconds of CPU time for solution.
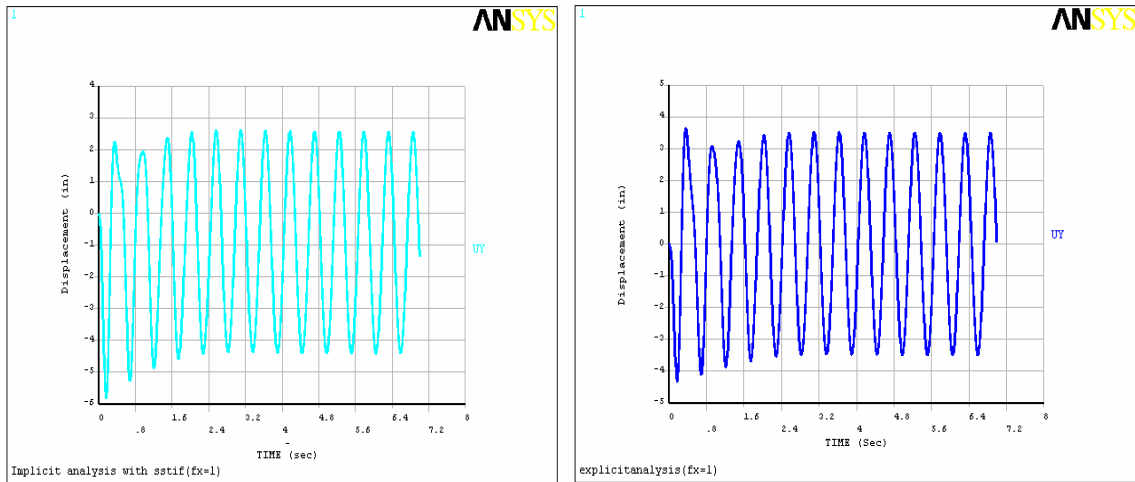
(a)   (b)

Figure4.6: Amplitude response obtained from a) implicit method b) explicit method for

lateral harmonic excitation and axial step load (1 *lb*) at free end

Figure4.7: Schematic diagram for Cantilever beam subjected to harmonic excitation and

step load (10 *lb*)

41

Figure(4.8) shows lateral free end response obtained from explicit finite method and implicit finite method for vertical harmonic load of F_L= 1 sin (w$_1$t) and step load of step load of 10lb in axial direction. The implicit method only took 270 sec of CPU time for solving on a computer (Pentium IV (2.8GHz) Main memory 512MB), while the explicit method took 401 seconds of CPU time for solution. Implicit finite element method and explicit dynamics finite element method generated the same steady state response amplitude. The steady state values obtained by both methods was 1.6254 in.

(a)   (b)

Figure4.8: Amplitude response obtained from a) implicit method b) explicit method for lateral harmonic excitation and axial step load (10 lb) at free end

Figure (4.9) shows lateral free end response obtained from explicit finite method and implicit finite method for vertical harmonic load of F_L= 1 sin (w$_1$t) and step load of step load of 25 lb in axial direction. Figure (4.10) shows lateral free end response obtained from explicit finite method and implicit finite method for vertical harmonic load of F_L= 5 sin (w$_1$t) and step load of step load of 25lb in axial direction.

$$F_L = 1 \times \sin(w_1 t)$$

$F_A = 25\,lb$
(Step load)
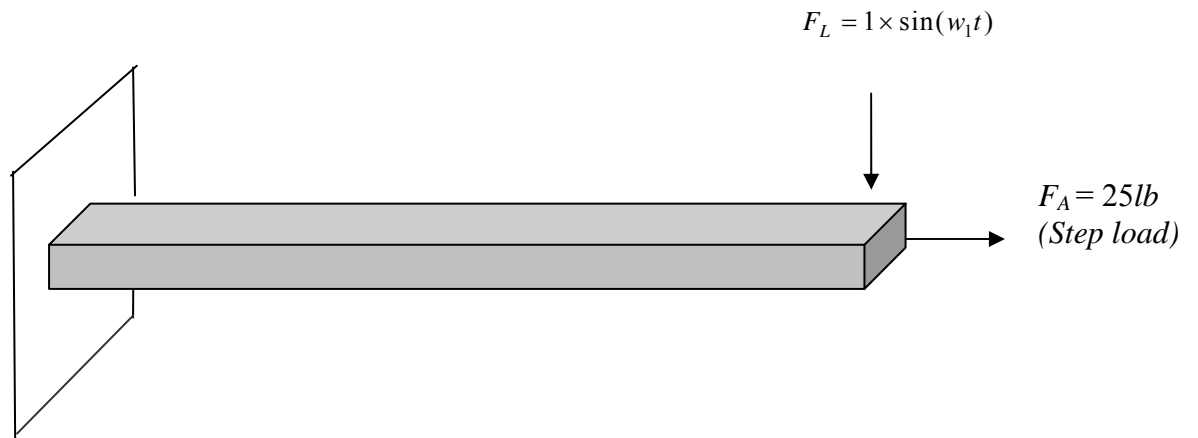
Figure 4.9: Schematic diagram for Cantilever beam subjected to harmonic excitation and

step load (25 *lb*)

The implicit method only took 248 of CPU time for solving on a computer (Pentium IV

(2.8GHz) Main memory 512MB), while the explicit method took only 395 seconds of

CPU time for solution. The steady amplitude obtained from the implicit method and

explicit methods are equal, and its value was 0.8702 in.

(a)   (b)
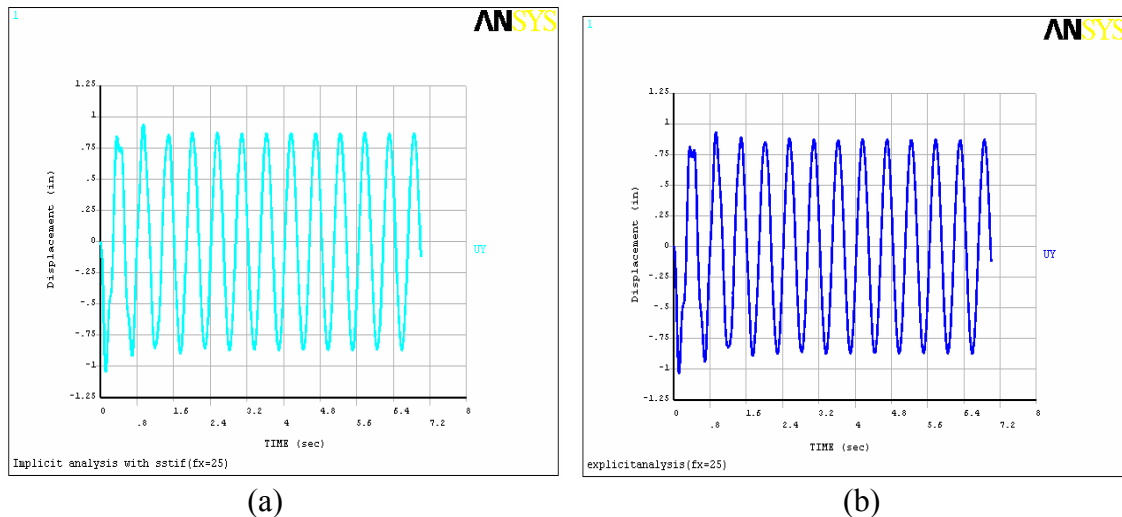
Figure4.10: Amplitude response obtained from a) implicit method b) explicit method for

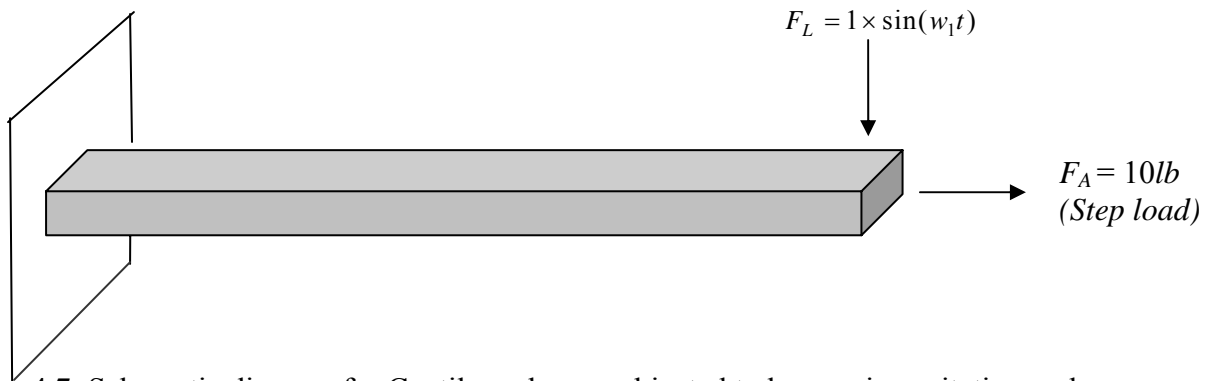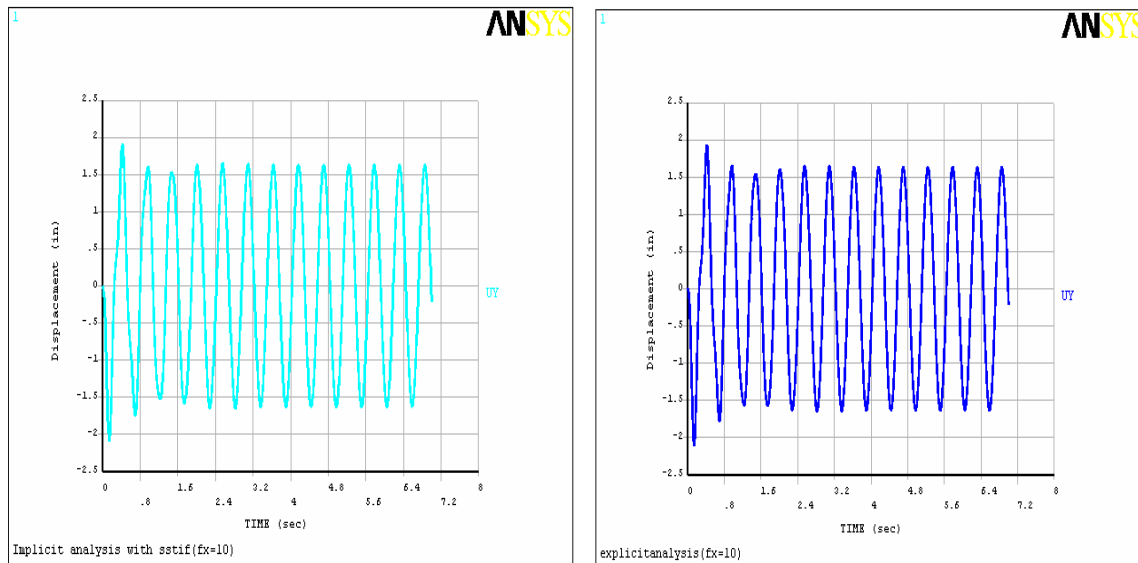lateral harmonic excitation and axial step load (25 *lb*) at free end

43

4.3 Nonlinear Beam Response Studies Using Implicit Finite Element Method

Figure 4.11 shows a schematic diagram of a flexible carbon steel cantilever beam subjected to axial base parametric excitation, described in references [5, 4]. The flexible cantilever beam is mounted vertically on a mechanical shaker, which provides vertical harmonic axial excitation. The focus of this study is to relate Anderson's experimental work and Kuiyin Mei's finite element analysis

$$x = \overline{X} \sin(wt + \phi)$$

$$V_0$$

$$y = \overline{Y} \sin(2wt)$$

Base
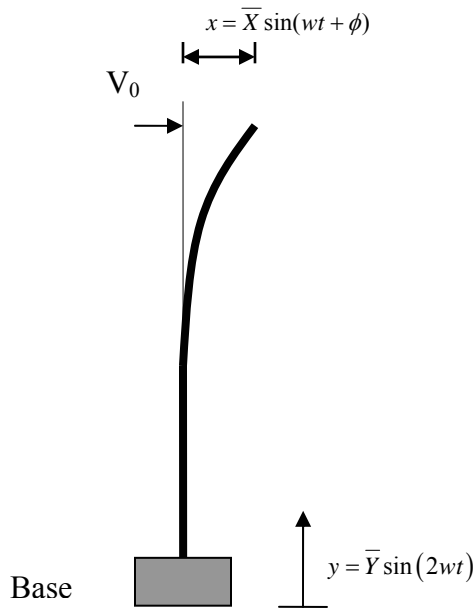
Figure 4.11: Schematic diagram of parametrically excited beam

Kuiyin Mei simulated the transient response of a flexible cantilever beam for first mode excitation using the explicit solver of ANSYS/LS-DYNA. The dimensions of the flexible cantilever beam are $33.56 \times 0.75 \times .032$ inches. The material properties of the beam are shown in the table (4.3). In this section, the beam response was simulated for principle parametric resonance of the first mode using the implicit solver of ANSYS.

Table 4.3: Material properties and input amplitude of FEA model of reference [4]

Young's Modulus (E)	30×10^6 lb/in^2
Density (ρ)	0.00073 lb.s^2/in^4
Possion's ratio (γ)	0.29
Amplitude of input acceleration (a)	46.53 in/s^2

The first four natural frequencies of this flexible cantilever beam, available in the literature, are 0.637 Hz, 5.61 Hz, and 16.10 Hz. A vertical axial harmonic excitation at the base is assumed. The excitation is an imposed displacement, with amplitude that depends on excitation frequency, applied at the base. The acceleration imposed at the base is constant for any excitation frequency, and the assumed value for the constant acceleration is 46.53 in/s^2. The beam is subjected to an initial condition of a small transverse velocity (0.5 in/sec) at its free end, as reported in reference [4].

ANSYS version 7.1 was used to simulate the nonlinear transient response for this case. 10 nodes and 9 elements of the ANSYS Beam3 element were used for modeling the beam. Geometric nonlinearities, stress stiffening and gravity effects were included in the analysis. The ANSYS command 'nlgeom' includes large deflections, and by default, it also includes stress stiffening effects in the analysis. An initial time step of 0.001 sec is selected for the analysis. Automatic time stepping is activated in the analysis to allow ANSYS to adjust the time step to avoid convergence problems. The 'AUTOTS' command activates automating stepping in the analysis. Damping of 0.32 percent of critical for the first mode of vibration is assumed in the analysis. This value is reported in

Reference [4]. The corresponding values of mass matrix multiplier, α , and stiffness matrix multiplier, β , are α =0.0015 and β = 0.0015. Figure (4.12) shows vertical base axial excitation as a function of time for the first 10 seconds, with an input frequency of 1.26 Hz .The excitation frequency is near twice the first natural frequency. Figure (4.13) shows lateral free end response obtained for axial base excitation frequency 1.26 Hz.
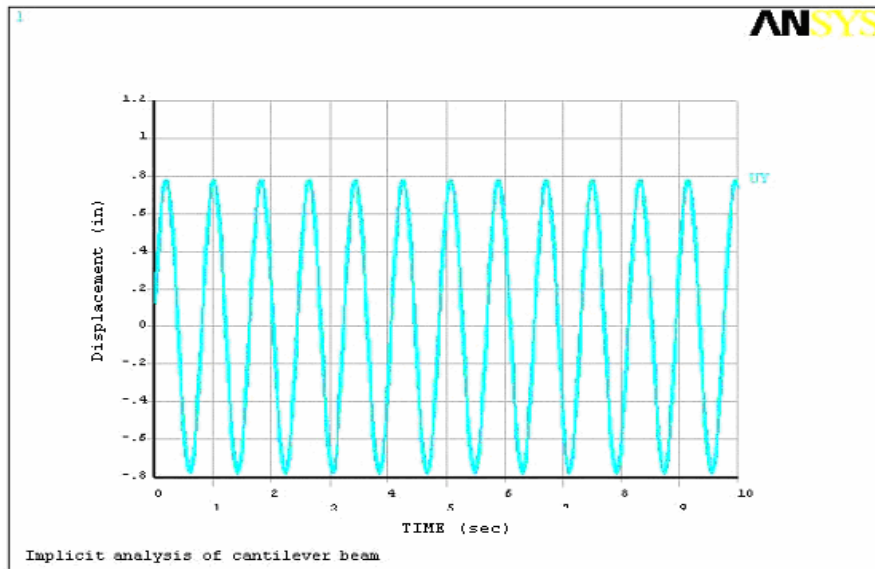
Figure (4.12): Axial base excitation with *f=1.26 Hz*
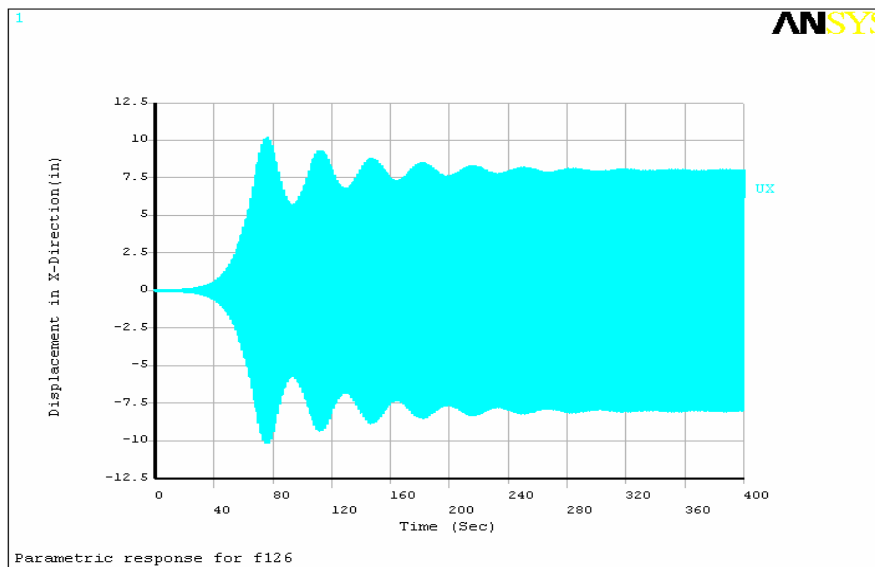
Figure (4.13): Lateral free end response for *f=1.26 Hz* by Implicit method

46

For a better understanding of this nonlinear beam response, the lateral free end response and axial base excitation results are plotted on the same graph in Figure 4.14 for the last 10 seconds (390-400 seconds) of the 400 second transient simulation.
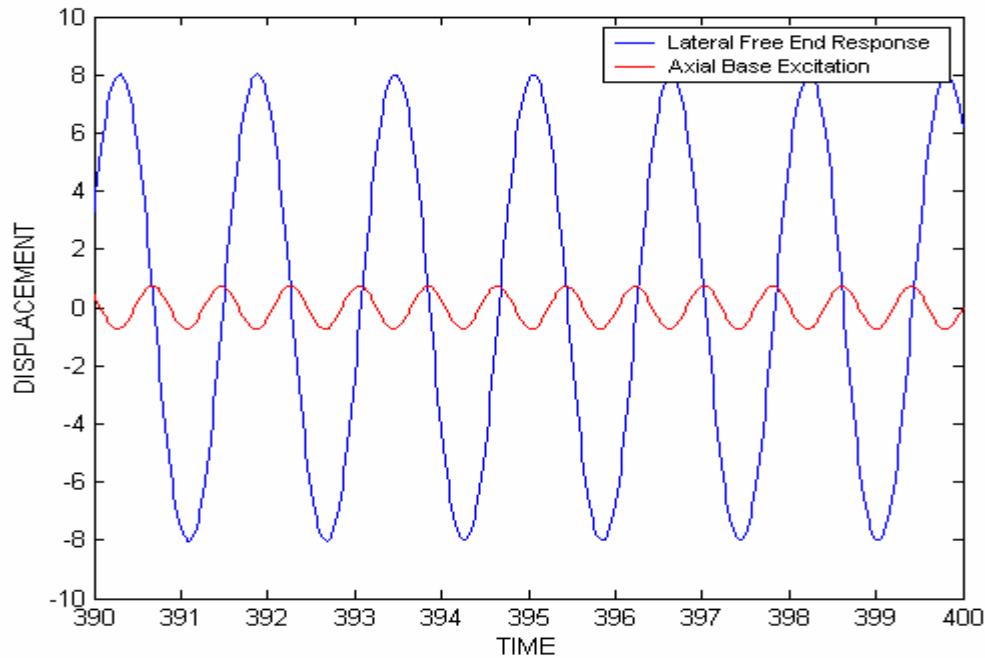
Figure 4.14: Lateral free end response for axial excitation frequency f=1.26 Hz

Figure (4.14) clearly shows that there are approximately 12.6 cycles of axial base excitation displacement for 10 seconds (390- 400 seconds) and approximately 6.5 cycles of lateral free end response for 10 seconds. Therefore, the free end of the flexible cantilever beam is oscillating with a frequency which is half of the axial base excitation frequency. Hence, the response of the beam is "parametric". Therefore, the ANSYS implicit solver has a capability to predict steady state parametric response for axial base excitations. Figure (4.15) presents the response of the free end of the beam for an axial excitation frequency of 1.3 Hz, with damping corresponding to α=0.0015 and β=0.0015. Figure (4.16) shows the lateral free end of the beam for axial base excitation

47

frequency 1.3 Hz with damping corresponding to α =0.0045 and β =0.0045. Comparison of Figure 4.15 and Figure 4.16 shows that increasing of damping not only decreases steady state amplitude, but also decreases the time taken for the beam to reach steady state. This increase in damping brings the response to steady state at 160 sec compared to about 300 sec for more lightly damped case.
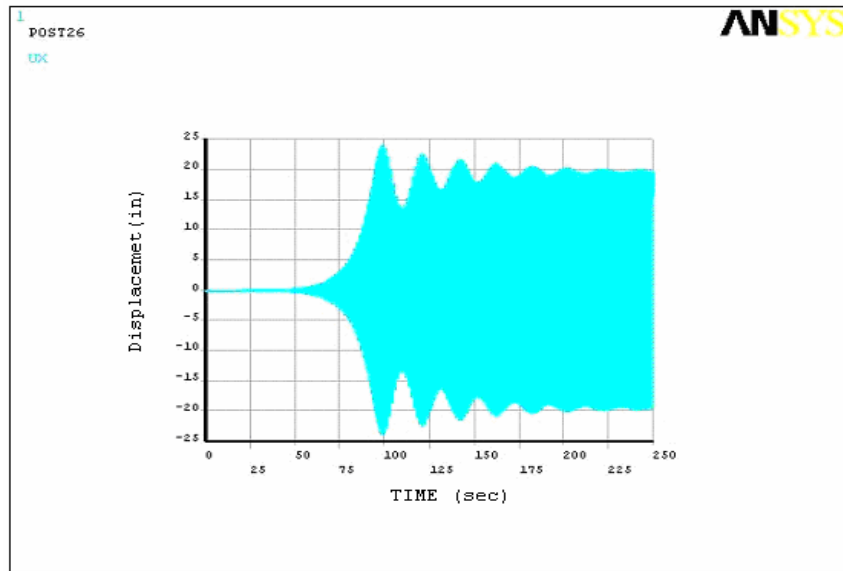
Figure 4.15: Lateral Free end response for *f=1.30 with* α =0.0015 and β =0.0015
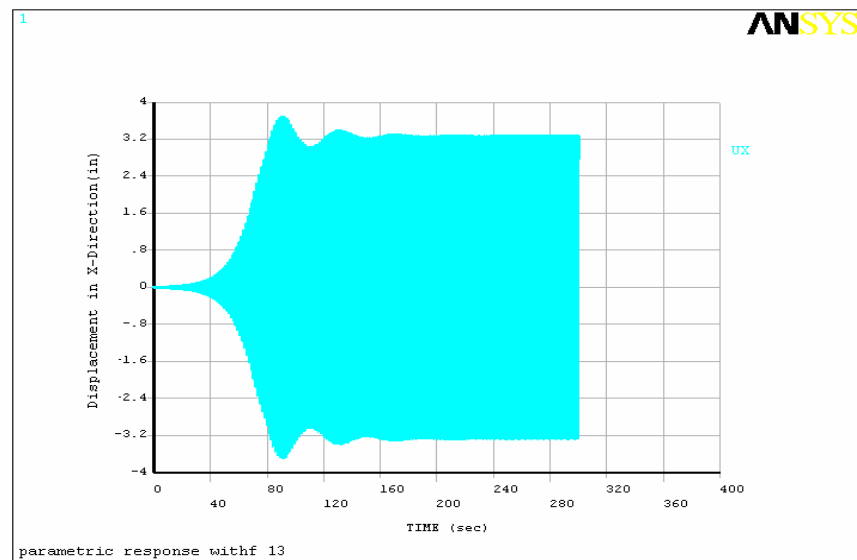
Figure 4.16: lateral Free end response for *f=1.30 with* α =0.0045 and β =0.0045

Figure (4.17) presents the response of the fee end of the beam for axial excitation frequency 1.24 Hz, with damping corresponding to α =0.0015 and β =0.0015. Figure (4.18) shows the response of the free end of the beam for axial excitation frequency 1.24 Hz, with damping corresponding to α =0.0045 and β =0.0045.
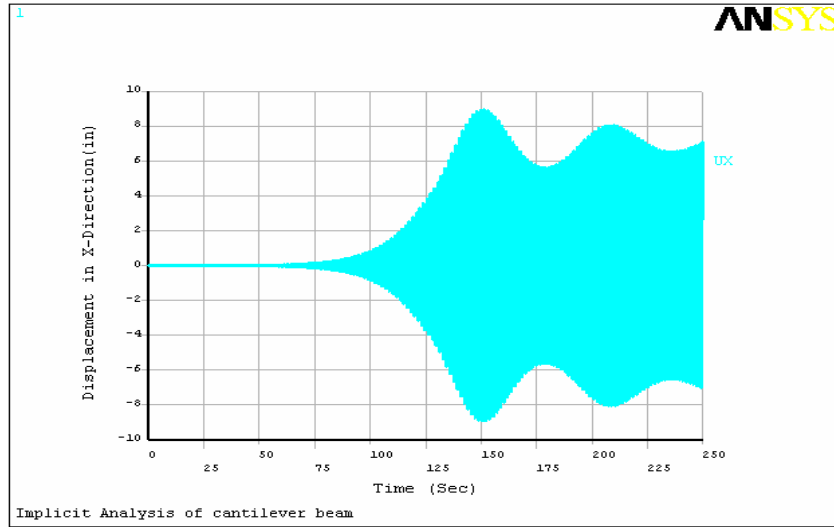
Figure 4.17: Lateral Free end response for *f=1.24 with* α =0.0015 and β =0.0015
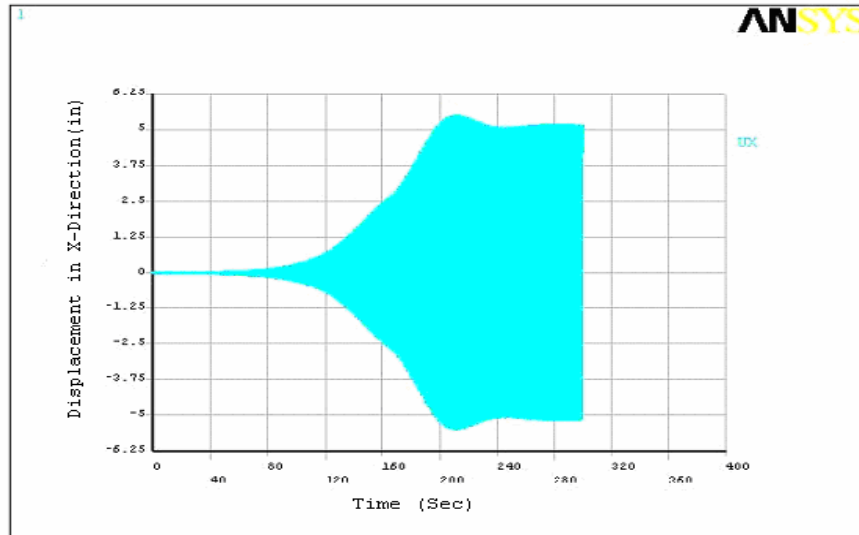
Figure 4.18: Lateral Free end response for *f=1.24 with* α =0.0045 and β =0.0045

4.4 Nonlinear Beam Response Studies Using Explicit Finite Element Method

Explicit finite element analysis was also performed to predict nonlinear response of cantilever beam as shown in the Figure 4.11 for axial base excitation. ANSYS/ LS-DYNA was used for the explicit finite element analysis. All the assumptions for the explicit dynamic analysis of the cantilever beam in the reference [4] were again considered here to make a comparison between implicit finite element analysis and explicit finite element analysis in terms of computational cost, accuracy, and stability. The cantilever beam was modeled with the Beam161 element. The finite element model has 10 nodes and 9 elements. The beam dimensions and material properties were given in the previous section

Figure (4.19) shows the free end response of the beam for an axial excitation frequency of 1.3 Hz with damping (α =0.0015 and β =0.0015), based on the explicit finite element method.
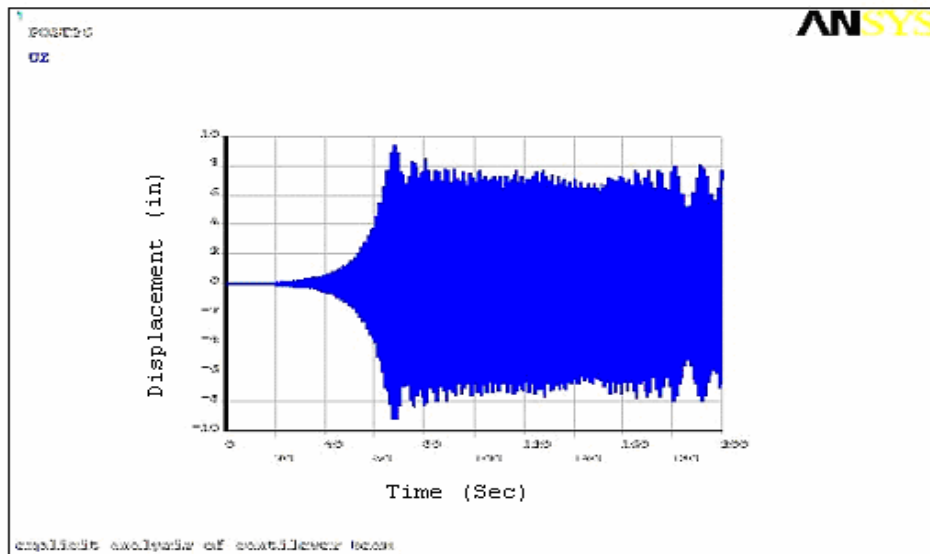
Figure 4.19: Lateral Free end response for axial frequency f=1.30 Hz by explicit method

Comparison of beam response by implicit finite element method and explicit finite method for excitation frequency f=1.30 Hz with modal damping of 0.32 percent of critical of the first excitation shows that the beam response obtained from the explicit method (Figure 4.19) has a comparable response amplitude to that obtained from the implicit method (Figure 4.15).   But, for the explicit solution, with the modeling assumptions used in this study, the explicit solution has not clearly reached a definite steady state, constant amplitude behavior. It appears that near the end of the simulation, some fluctuations of the amplitude of the response are occurring.

Figure (4.20) shows the free end response of the beam for an axial excitation frequency 1.24 Hz, with damping (α =0.0015 and β=0.0015)
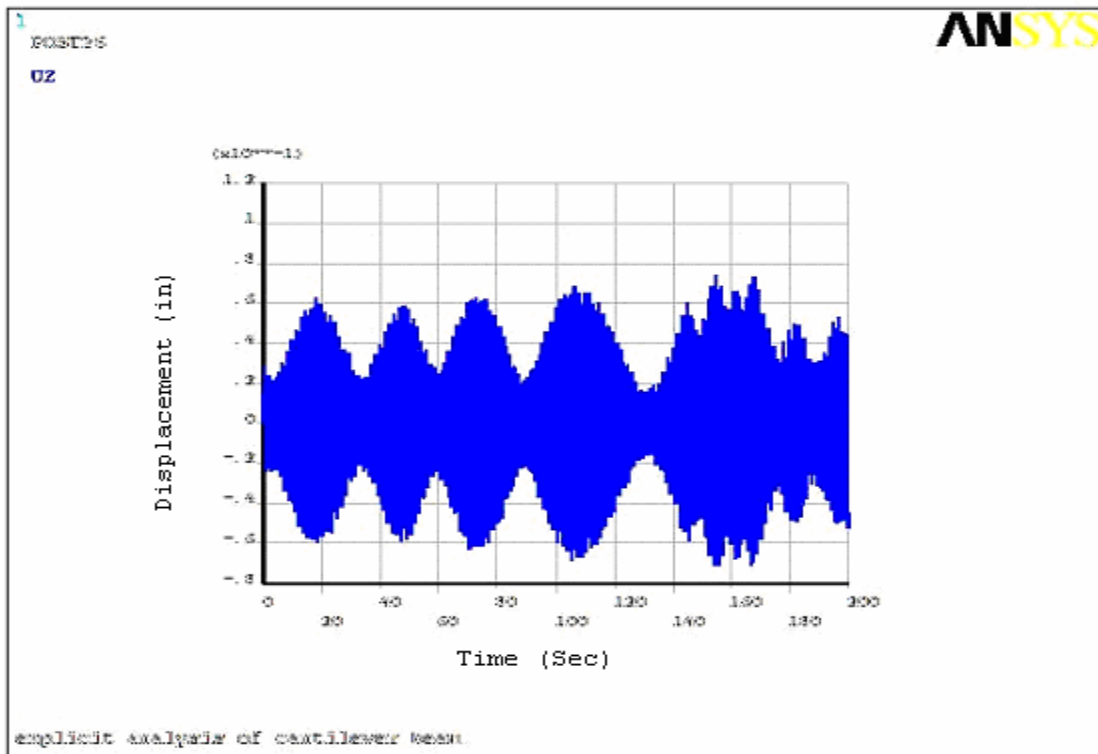
Figure 4.20: Lateral response for axial frequency f=1.24 Hz by explicit method

By using the command 'EDCTS' in ANSYS/LS-DYNA, the scale factor for the computed time step for an explicit dynamics analysis can be altered. Therefore explicit dynamics finite element analysis can be performed with different time steps using the EDCTS command. Hence, explicit dynamics finite element analysis was performed with different time steps, along with various damping levels, to attempt to generate a clear steady state solution.

Different time steps and various damping values which were attempted, but did not generate a clear steady state response for an axial base excitation frequency 1.23 Hz can be summarized as:

1. Changed time step from default of 0.9 to 0.1 with modal damping corresponding to α =0.0015 and β =0.0015.

2. Increased modal damping corresponding from α =0.0015 and β =0.0015 to α =0.0045 and β =0.0045, and time step scaling factor was changed to 0.05 from default value of 0.9.

3. Applied alpha damping only, with mass matrix multiplier, α =0.0045, and time step scaling factor of 0.01.

4. Applied alpha damping only, with mass matrix multiplier of α =0.123, and time step scaling factor of 0.01.

5. Applied alpha damping only, with mass matrix multiplier of α =0.615, with time step scaling factor of 0.05.

Further, an additional study was carried out for axial base excitation frequency 1.24 Hz, in which alpha damping only was assumed and three different mass matrix multipliers were assumed: α =0.08168, 0.20420, and 0.4084. In all three of these cases, the time step scaling factor assumed was 0.01. None of these three cases yielded clear steady-state response amplitude.

4. 5 Summary of Example Studies

There was good agreement obtained in the studies of Section 4.2 for beam response due to lateral loading between the explicit and implicit analysis methods. An exhaustive study, involving extensive variations of time step parameters and other modeling parameters, to decisively conclude which method was most computationally efficient, was not undertaken. But, from the results, it appears that both methods produce basically the same results in terms of beam response for a given set of loading and damping assumptions. Agreement was obtained even for cases involving stress-stiffening and large deflections.

However, in the case of nonlinear lateral parametric response due to axial base excitation, as outlined in Section 4.3, although the response results were comparable for an excitation frequency of 1.30 Hz, the results from the implicit simulation appeared to produce a clearer steady-state condition, which might be expected under the applied loading, than that produced by the explicit dynamics method. For other excitation frequencies considered (1.23 Hz and 1.24 Hz), based on the modeling assumptions in this study, clear steady-state response amplitude was even more difficult to ascertain from the

explicit dynamics solutions. Certainly, more study could be undertaken in an attempt to improve the results from the explicit dynamics solutions by modifying other modeling parameters. But, the primary goal of this thesis was to determine procedures for implementing quadratic damping for cases with axial excitation like that in the simulations of Section 4.3. The determination of better methods for using explicit dynamics in the study of parametric response of beams is left in this work as a suggested area for further study.

Because the implicit analysis method seemed to more easily produce results with a clear steady-state lateral response amplitude for cases of axial excitation of the flexible beam being considered, it was decided that quadratic damping studies would be implemented in this work based on the implicit dynamics method.

CHAPTER 5

TRANSIENT SIMULATIONS WITH QUADRATIC DAMPING

5.1 INTRODUCTION

Damping in any form results in energy loss in any dynamic system, which leads to decay of amplitudes of motion [29]. As mentioned in Chapter 1, when a body moves through a fluid (air), the damping force due to fluid resistance is proportional to the velocity of the moving body at low Reynolds numbers, whereas at high Reynolds numbers, the damping force is proportional to the square of the velocity. Anderson's [5] theoretical and experimental studies on nonlinear response of a flexible cantilever beam for axial base excitation concluded that inclusion of quadratic damping along with linear structural damping in an analysis improved agreement between experimental and theoretical results for first mode response of the beam's parametric vibration. Therefore, in this work the "velocity–squared" damping was applied, along with linear structural damping in the transient simulations of a flexible cantilever beam for first mode response to parametric axial excitation using the commercial finite element code, ANSYS. The different types of damping options preprogrammed in ANSYS are mass-proportional, stiffness-proportional, and modal damping. There is also a user-option in ANSYS to implement a coefficient for "velocity-squared" damping using the ANSYS Combin14 element.

However, a different, more flexible approach is developed and implemented in this work. Based on ANSYS parametric design language (APDL), a method is developed for including the velocity squared damping assumption in the transient dynamic analysis of a flexible cantilever beam. This method allows for the damping force to remain normal to the beam for large deflections, and could be easily adapted for alternative damping assumptions. The following section describes implementation of velocity squared damping, and an overview of nonlinear transient simulation procedure using ANSYS.

Based on the studies of Chapter 4, the implicit method appears to produce results with more stable steady-state solutions for lateral parametric response to axial excitation. While, as discussed in Chapter 4, further study may reveal modeling procedures that result in comparable results using the explicit method, it was decided in this work to implement the quadratic damping using the implicit method.

5.2 Overview of Simulation Procedures using ANSYS

Nonlinear response of a flexible cantilever beam [4, 5], corresponding to first mode motion, is simulated for axial base excitation with a frequency near twice the first natural frequency, including quadratic damping using ANSYS. The beam has dimensions $33.56 \times 0.75 \times .032$ inches, and its material properties are given in the Table (4.3). The Beam3 element of ANSYS is used to model the beam. The beam is subjected to an imposed axial base harmonic displacement with an excitation frequency equal to approximately twice the first natural frequency. Consistent with the work in Reference [4], the amplitude of input acceleration assumed is 43.56 *in / s²*. As an initial condition,

the free end of the beam is subjected to a transverse initial velocity of 0.5 in/sec. The "full" method option of transient dynamic analysis in ANSYS is selected for the transient simulations, and this is specified by using the command 'ANTYPE, trans'. The command, 'IC', is used to input the initial transverse velocity at the free end of cantilever beam. The base of the cantilever beam is constrained to zero translation in the y-direction, and zero rotation about the z-axis. The imposed harmonic displacement is in the x-direction (axial direction).

Because the axial base parametric excitation of the flexible cantilever beam can lead to large deflections, geometric nonlinearities must be included in transient dynamic analysis. The ANSYS command 'NLGEOM, on' activates geometric nonlinearities, which includes large deflection, large strain, and large rotation. The 'NLGEOM,on' command, by default activates stress stiffening effects in the analysis. Gravity effects are included in the analysis using the command 'ACEL'.

Velocity-squared damping can be implemented in a transient analysis of a beam by retrieving values of displacements and rotations at each node at the end of the solution for successive small time intervals. Based on the displacements at the end of one time interval, and the displacements stored at the end of the previous time interval, corresponding velocities are calculated at each node. From the obtained velocities at each node, a damping force can be calculated at each node by assuming a constant quadratic damping coefficient and multiplying with the square of the velocity. Then the calculated damping force at each node is included in the analysis by explicitly defining forces at

each node for the next small time interval and the process is repeated for the duration of the analysis. During a given small time interval, the damping forces are assumed constant. But, if the time interval utilized is sufficiently small, then the procedures should produce results that approximate the real-world situation of continuously varying damping forces.

For a better understanding of implementation of quadratic damping in ANSYS, the lateral displacement of a cantilever beam due to axial excitation is considered. Figure (5.1) shows a schematic diagram for parametric response of a flexible cantilever beam with the x and y directions shown along with the normal, *n,* and tangential, *t,* directions. The angle between the *x* and *t* direction is θ . Assume v_x and v_y are the components of nodal velocities in *x* and *y* directions, respectively, and v_t and v_n are the components of nodal velocities in the tangential and normal directions, respectively. Using a coordinate transformation, we can find the corresponding normal and tangential components of the nodal velocities from the nodal velocities in the x and y directions.

$$\begin{bmatrix} v_t \\ v_n \end{bmatrix} = \begin{bmatrix} \cos\theta & \sin\theta \\ -\sin\theta & \cos\theta \end{bmatrix} \begin{bmatrix} v_x \\ v_y \end{bmatrix} \qquad (5.1.1)$$
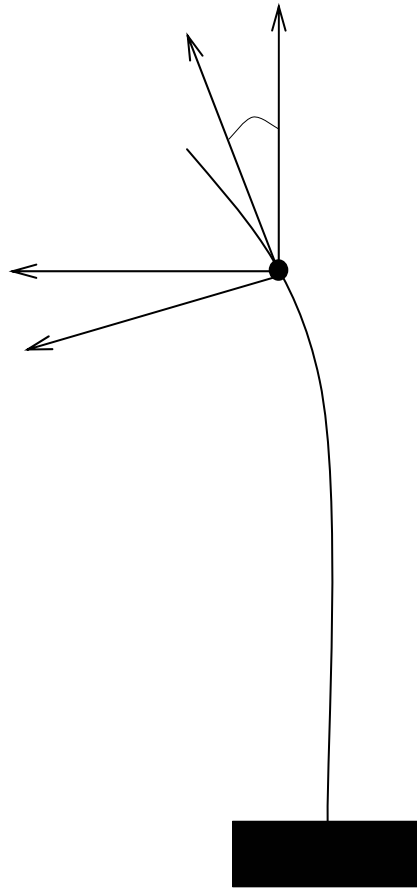
Figure 5.1: Schematic diagram of a beam with normal and tangential components of

damping force

Equation (5.1.2) gives the relationship between nodal damping forces due to fluid

resistance in the normal direction of the beam at some node along the beam:

$$f_d = -Dv_n |v_n| \qquad (5.1.2)$$

Where

f_d = Nodal quadratic damping force

v_n = Normal component of nodal velocity.

D = Quadratic Damping Coefficient;

The quadratic damping force is positive when $v_n < 0$ and negative when $v_n > 0$. As it seems reasonable that the fluid resistance acts in the direction normal to the beam's lateral displacement in the parametric response of flexible cantilever beam, we will assume that the quadratic damping force f_d acts in the normal direction. We can write,

$$\begin{bmatrix} (f_d)_x \\ (f_d)_y \end{bmatrix} = \begin{bmatrix} \cos\theta & -\sin\theta \\ \sin\theta & \cos\theta \end{bmatrix} \begin{bmatrix} 0 \\ f_d \end{bmatrix} \qquad (5.1.3)$$

Therefore using equations (5.1.3) we can calculate the x and y components of the quadratic damping force. Hence, if we know the instantaneous nodal velocities, the nodal quadratic damping forces are,

$$(f_d)_x = (-\sin\theta) f_d \qquad (5.1.4)$$

$$(f_d)_y = (\cos\theta) f_d \qquad (5.1.5)$$

The ANSYS Parametric Design Language command, "*get", retrieves data from the database of calculated results, or data related to previous user input, either as a scalar parameter or in used-defined array parameters. The "* get" command can also be used to obtain values from preprocessing, solution, and post processing, corresponding to nodes, elements, keypoints, areas, volumes etc. Therefore, in the transient simulation of parametric response of a flexible cantilever beam, the * get command is used, along with a do-loop (implemented with the APDL '*do' command) to obtain within the ANSYS

post processor the nodal displacements and rotations, with respect to the global x-axis, at each node of the beam, at the end of each small time interval

At the start of the solution, the displacement in the x and y direction at each node is assumed zero, and stored in scalar parameters, 'uxold', and, 'uyold', respectively. The transient dynamic analysis is performed for an initial small time interval. After completion of the solution at the end of this initial time interval, from the general postprocessor of ANSYS, the '*get' command is used, along with a do-loop to obtain components of nodal displacements in the x and y directions, and rotation about the global z-axis. The corresponding displacement and rotation values obtained from each node of the flexible cantilever beam are stored in new scalar parameters, 'uxnew', 'uynew', and 'phi', respectively. Therefore, from the newly obtained nodal displacements after a small interval, along with previously calculated nodal displacements from the previous time interval, components of velocities in the x and y directions at each node are calculated. Components of velocities at each node in the normal and tangential directions are obtained by coordinate transformation of components of nodal velocities in the global x and y directions using Equations (5.1.1). Then, the velocity-squared damping force at each node is calculated for a constant quadratic damping coefficient using equation (5.1.2), and transformed to corresponding velocity-squared damping forces in the x -direction and y -directions using Equations (5.1.3). After completion of the solution for the initial time interval, damping forces corresponding to quadratic damping at each node are calculated using the general postprocessor, and included in the analysis for the next time step.

Restarting of a full transient analysis can be done from the previous analysis time interval using the 'REST' option of the 'ANTYPE' command. By default, the restart option will activate a multiframe restart for a full transient analysis. A multiframe restart writes different files to the database, which is time consuming. Therefore, a singleframe restart is used, after completion of the solution for each time interval. The 'RESCONTROL' command can also be used to restart a transient analysis without activating a multiframe restart from the last load step, or from the point where the previous analysis was stopped. The 'RESCONTROL' command controls the multiframe restart of the analysis in terms of writing files to the database. Therefore 'ANTYPE, trans, rest', along with the command 'RESCONTROL, define, none, none', is used to activate singleframe restarting of transient analysis of the flexible cantilever beam from saved information of the previous time interval.

Hence, after finishing the solution for the initial time step, damping forces corresponding to nodal quadratic damping are calculated and applied in a restarted transient analysis. This process is repeated using a do-loop for the duration of the analysis. Alpha damping is included in the analysis, with a mass matrix multiplier, α, equal to 0.00001. Appendix C presents an ANSYS batch file corresponding to a transient finite element simulation of the cantilever beam subjected to axial base excitation including quadratic damping. The command 'OUTRES' writes the results from the solution to the database and the command '/CONFIG' controls the number of results sets allowed on the result file. By default '/CONFIG' allows for 1000 results sets to be written to the results file, and can be

increased to any required number. These two commands affect the solution time. Therefore, these commands must be used in accordance with user requirements. Hence, in the transient simulation of cantilever beam, the 'OUTRES' command is used to write results corresponding base and free end only, which is of interest in this analysis.

Figure5.2 shows lateral free end response obtained from transient analysis of the beam for axial base excitation including quadratic damping. The flexible beam is excited at a frequency of 1.27 Hz and the time interval selected for the solution is 0.001, with quadratic damping coefficient D=25e-7. It takes 23 hours of CPU time on a Dell 1.6 GHz, Pentium4 PC, with 1 GB RAM, to generate 125 seconds of transient response. Figure5.3 shows that lateral response has approximately 6.5 cycles for 10 seconds which is nearly half of the excitation frequency 1.27 Hz. Hence the response obtained is a parametric response. Figure 5.4 shows free end response of a 60 node beam model without any damping. Therefore, comparison of response obtained from no damping with quadratic damping shows quadratic damping is influencing the steady state response. Figure 5.5 shows free end response of a 60 node beam model with alpha damping only. Comparison of response obtained from no damping case with alpha damping (α= 0.00001) shows that applied alpha damping with the very small alpha value used, has negligible effect.
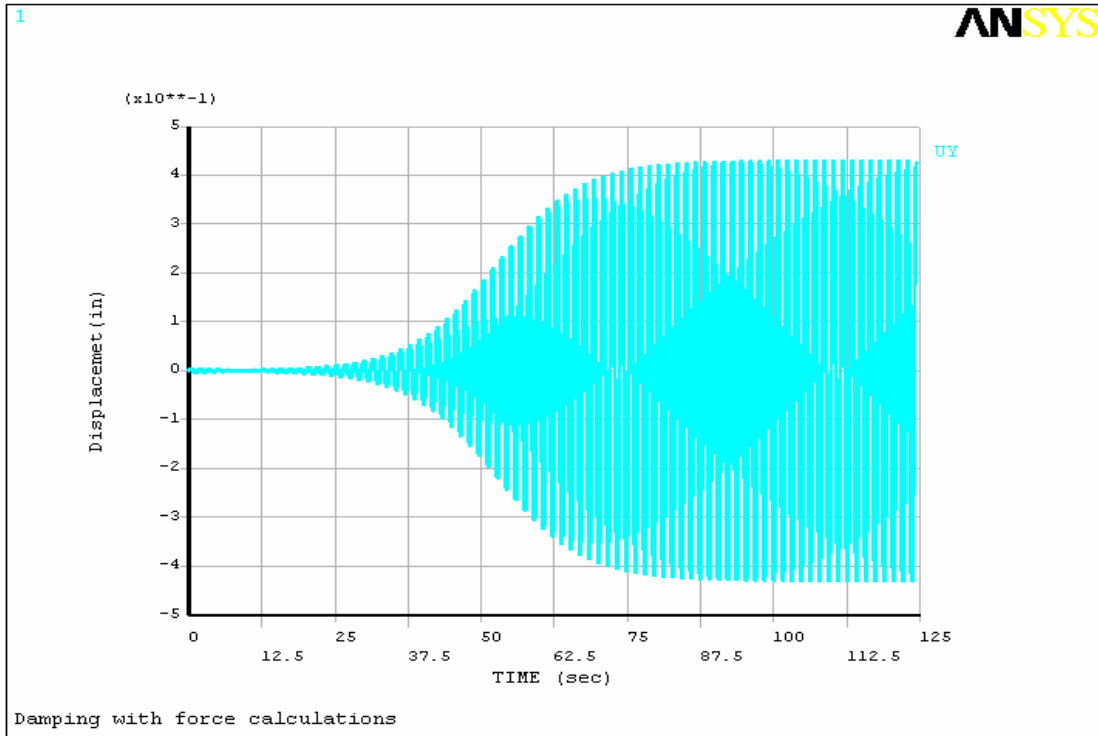
Figure 5.2: Lateral free end response for *f=1.27 Hz* including quadratic damping
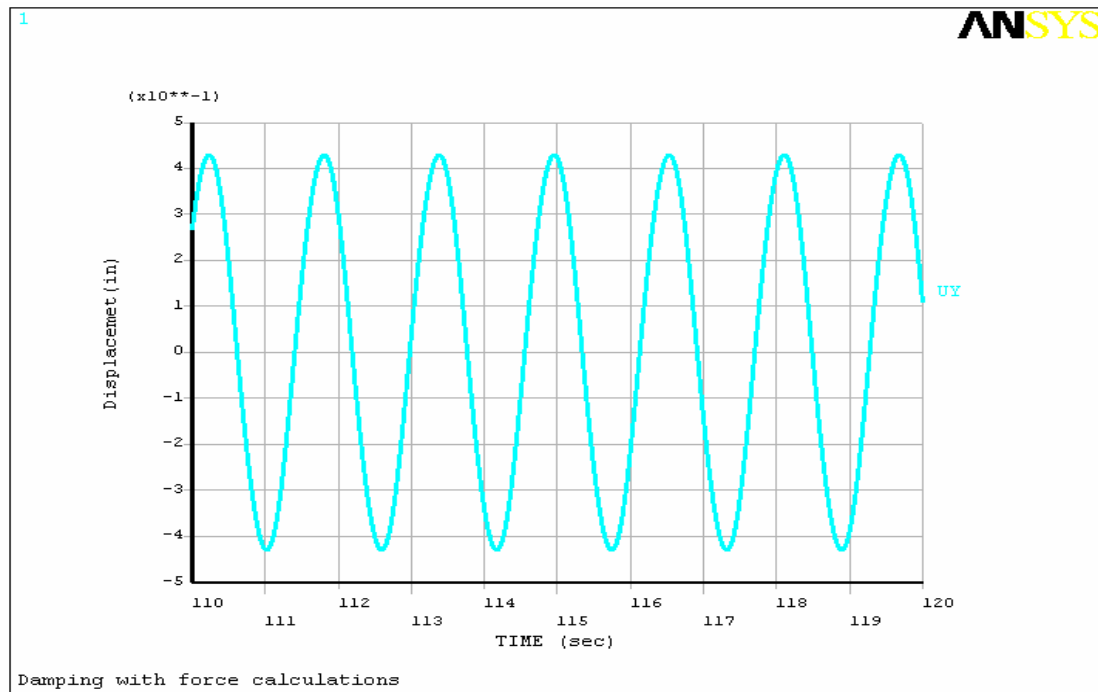
Figure 5.3: Lateral free end response for *f=1.27 Hz* for time range (110-120 sec)

including quadratic damping
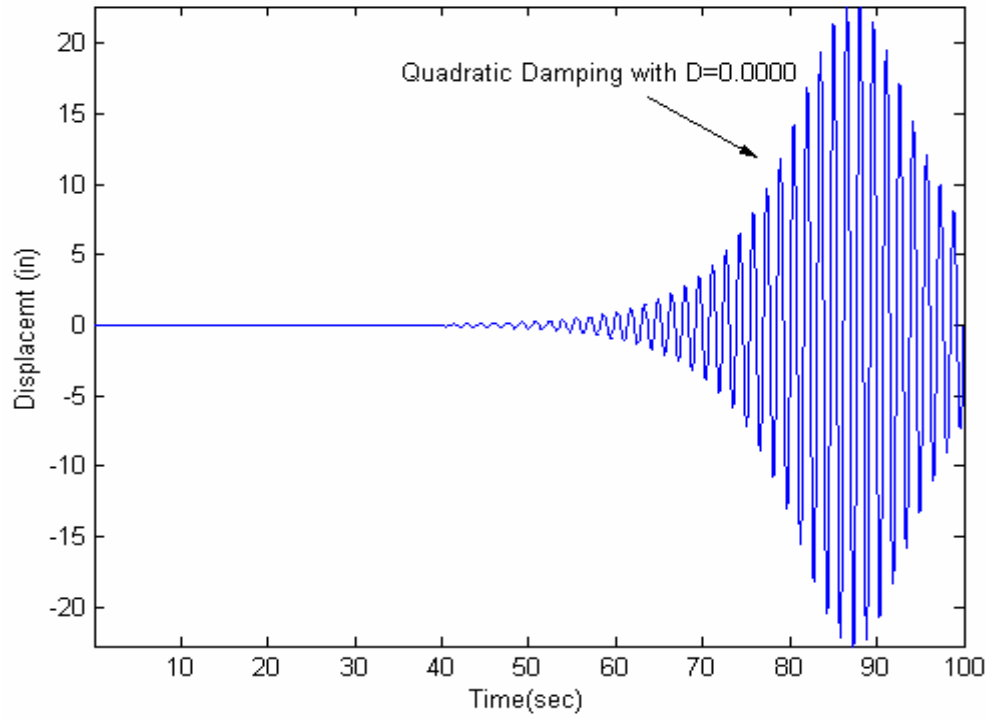
Figure 5.4: Free end response for *f=1.28 Hz* with Damping coefficient D=0.000
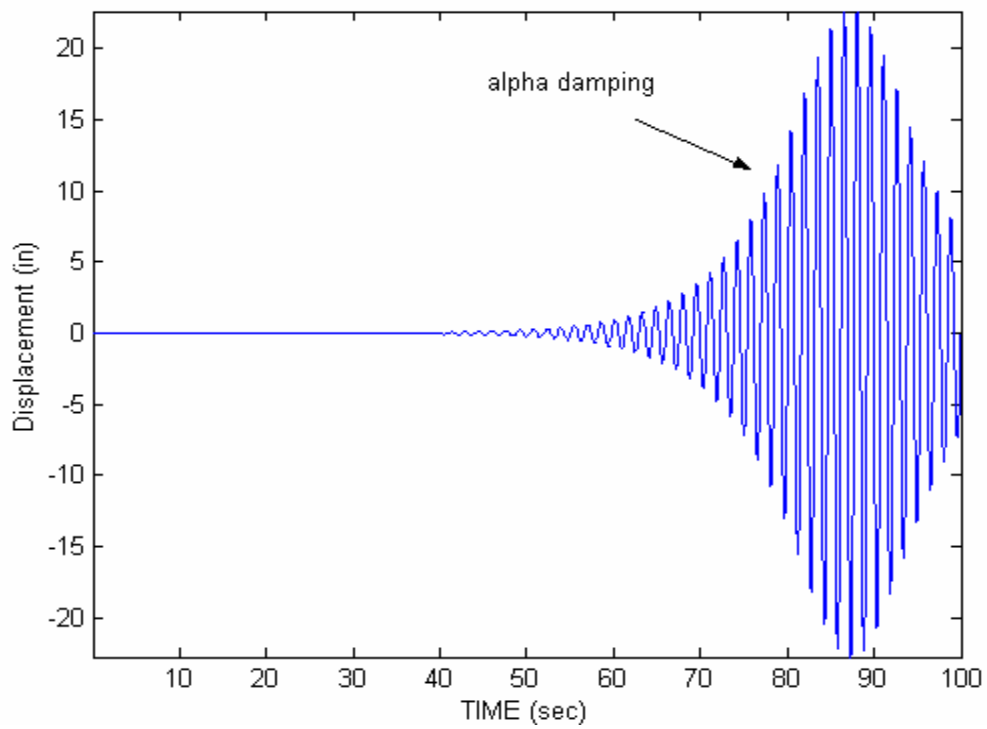
Figure 5.5: Free end response for *f=1.28 Hz* with alpha damping α=0.00001

5.2.1 A Study on Effect of Selected Time Interval

Transient simulation results were generated with an excitation frequency $f= 1.28\ Hz$ with quadratic damping coefficients $D=1e-6$, with time intervals 0.001, 0.002 and 0.0005 seconds, to determine a reasonable time interval for the analysis. The corresponding plots are shown in the Figures 5.7, for a time range 92.5-94 seconds
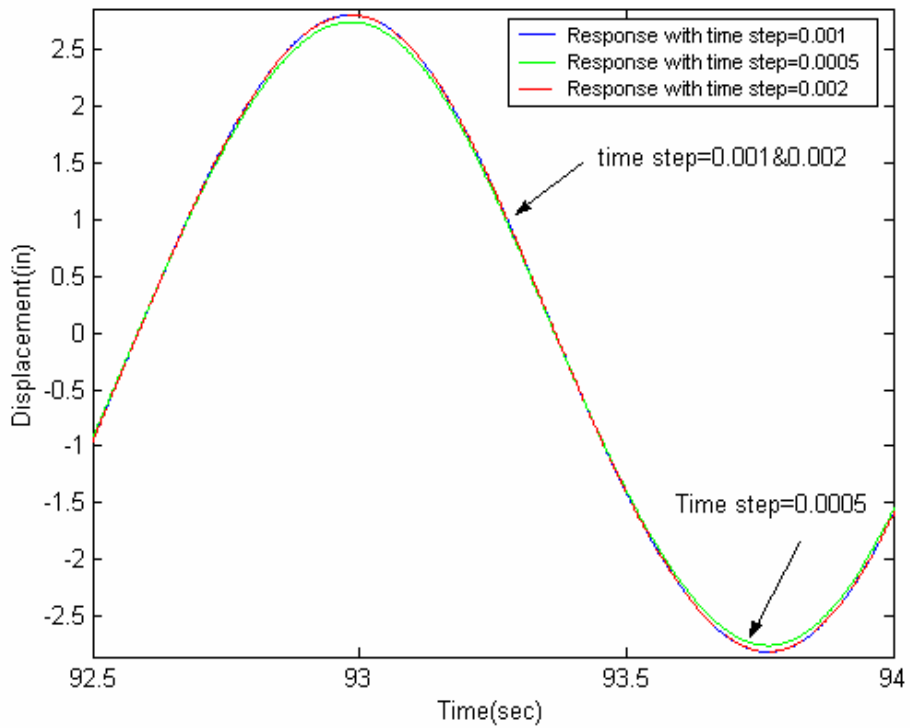
Figure 5.7: Lateral Free end response with excitation $f=1.28\ Hz$ with time intervals 0.001, 0.002, 0.0005 seconds.

Comparison of the lateral free end response obtained with time steps of 0.001, 0.002, and 0.0005 seconds shows that a 0.001 second interval is likely a reasonable time interval for the cases being studied. Clearly, there is approximately the same steady-state response amplitude for a 0.001 second interval as there is for a 0.0005 second interval. A smaller

interval should be better for approximating a continuously changing damping force, but the smaller the interval, the longer the solution time. In these studies, based on the results in this section, it was determined that a time interval of 0.001 seconds is probably sufficiently small to produce reasonable accuracy without excessive solution times.

5.2.2 Mesh Density Analysis

Additional nonlinear transient analyses were also performed with the beam using 20, 40, and 60 nodes, with a selected time interval of 0.001 seconds. Figure 5.8 compares lateral free end response for 20 nodes and 40 nodes for steady-state response in the time range of 95-100 seconds. The steady-state amplitude value obtained from 20 nodes is 3.4% greater than the steady-state amplitude of the 40 node case. Figure 5.10 compares lateral free end response for 20 nodes with that for 60 nodes, and Figure 5.9 compares the 40 nodes result with the 60 nodes result. The steady state amplitude value obtained from 20 node beam is 6.7% greater than the steady state amplitude of the 60 node model. The steady state amplitude value obtained from the 40 node model is 3.2 % greater than the steady state amplitude for the 60 node case. Figure 5.11 compares lateral free end response for 60 nodes with the result for 80 nodes. The steady state amplitude value obtained from 60 nodes is 2.34 % greater than the steady state value for 80 nodes. It appears that the results are likely nearly converged for a 60 node case, although further mesh refinement could produce somewhat better results at the expense of additional solution time.
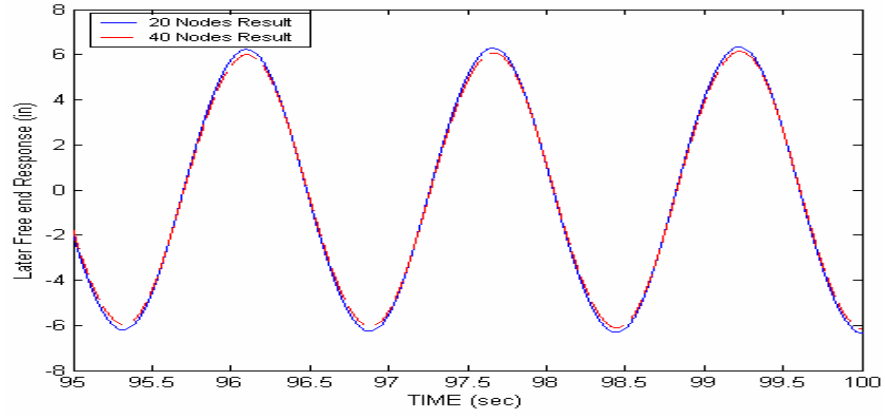
Figure 5.8: Comparison of 20 node model result with 40 node model result.
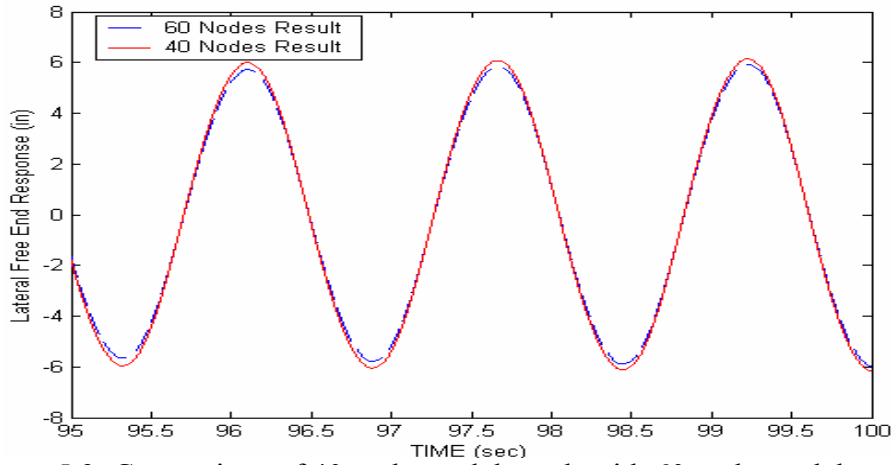
Figure 5.9: Comparison of 40 node model result with 60 node model result.
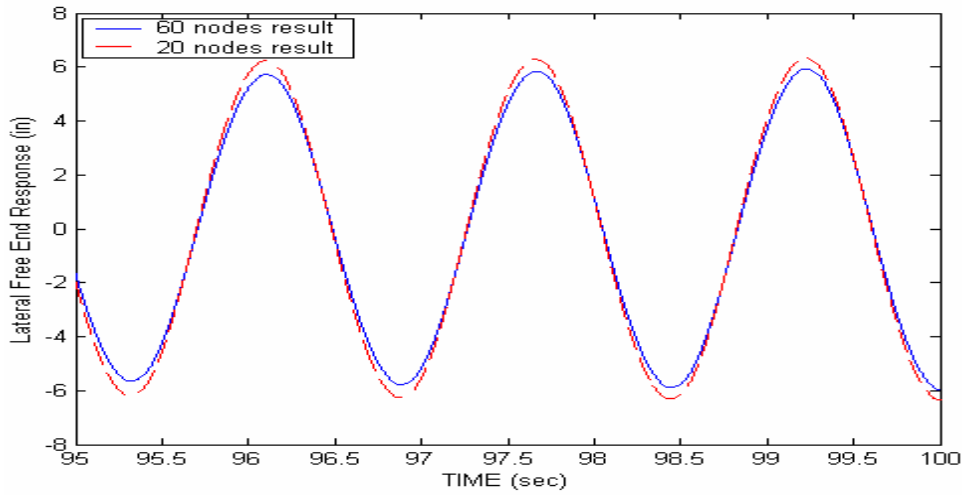
Figure 5.10: Comparison of 20 node model result with 60 node model result
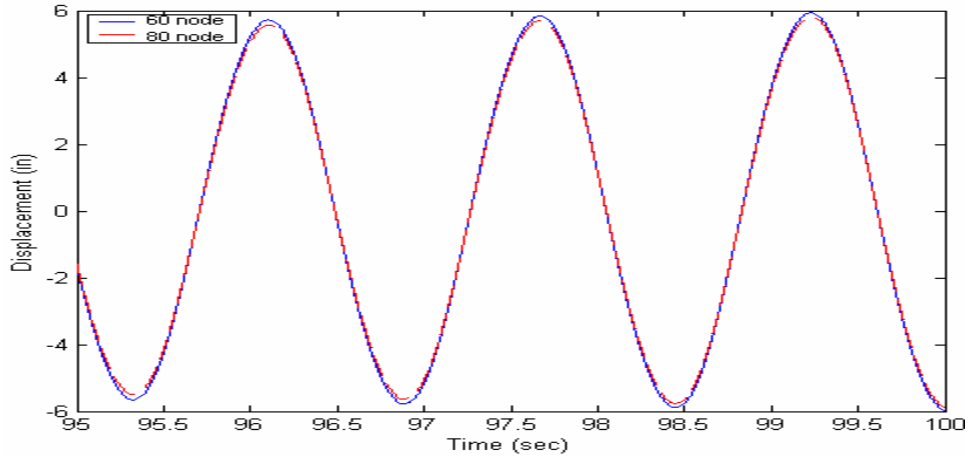
Figure 5.11: Comparison of 60 node model result with 80 node model result

5.3 Confirmation of Simulation Procedures

Two simple cases are considered to verify the simulation procedure implemented in ANSYS for nonlinear response of a flexible cantilever beam which includes quadratic damping by the calculation of damping force proportional to the square of velocity. For the two cases, response is compared for damping applied by a dashpot (Using Combin14 element) and by force calculations. The following sections give a complete description of the two cases.

5.3.1 CASE1: Spring-Mass System subjected Axial Harmonic Load

As a first case, a simple Spring–Mass Damper systems is considered which is subjected to axial harmonic excitation, and the response is compared for damping applied by using a the ANSYS Combin14 element and by using force calculations, in which damping is implemented in a manner similar to that outlined above, in which the solution is broken into numerous small time intervals, and damping forces are explicitly defined and assumed constant throughout a small time interval.

69
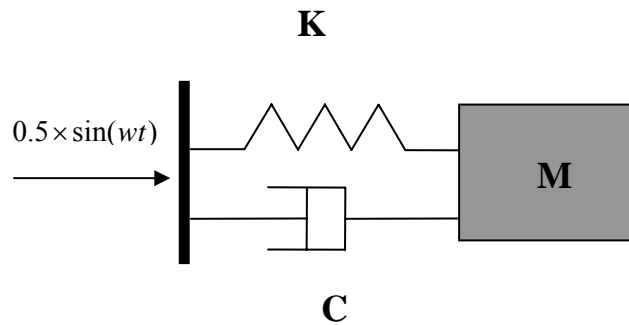
Figure 5.12: Single degree of freedom spring- Mass-Damper System

Figure 5.12 shows a single degree of freedom spring –mass-damper system subjected to harmonic excitation at the support. The assumed values for mass, m, spring constant, k, and damping coefficient, c, for the system are m=1 *lb, c=16.679 lb/in* and k=0.81679 *lb-s/in*. The spring is modeled using a Combin14 element, and the mass is modeled with Mass21 element. The Combin14 element of ANSYS is a spring-damper element. Combin14 can also be used to model a spring element with zero damping, or a damper (dashpot), with zero stiffness. Therefore, for the case of damping applied by force calculations (implemented as constant explicitly defined forces within each small time interval), the Combin14 element is simply a spring element zero damping. Figure 5.13 shows the response of the mass with damping applied by using a Combin14 element for 20 seconds. Figure 5.14 shows the response of the mass in the axial direction with damping applied by using force calculation, as described above. But in this "force calculation" case, damping is proportional to velocity, and not proportional to velocity-squared. So, the results in Figure 5.13 should be in agreement with those in Figure 5.14. Comparison of figure 5.13 with figure 5.14 shows that the response obtained from damping applied by using force calculations are nearly identical to the response obtained from damping applied with the Combin14 element.
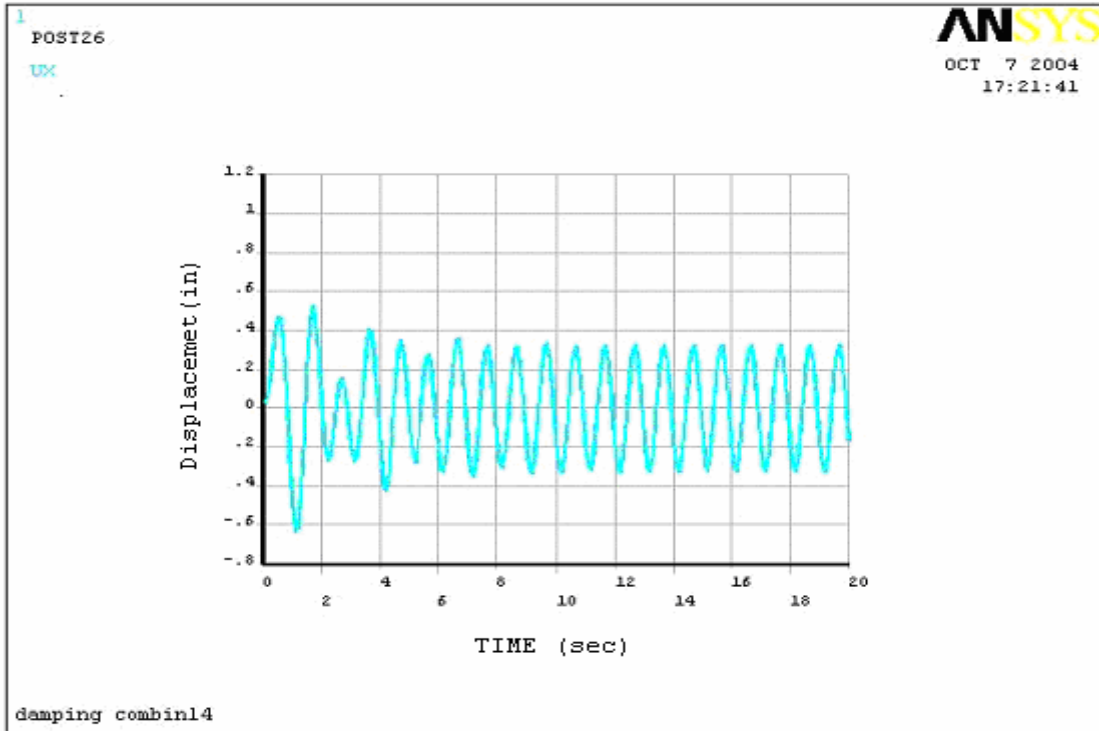
Figure 5.13: Axial response of the mass with damping by applied using Combin14
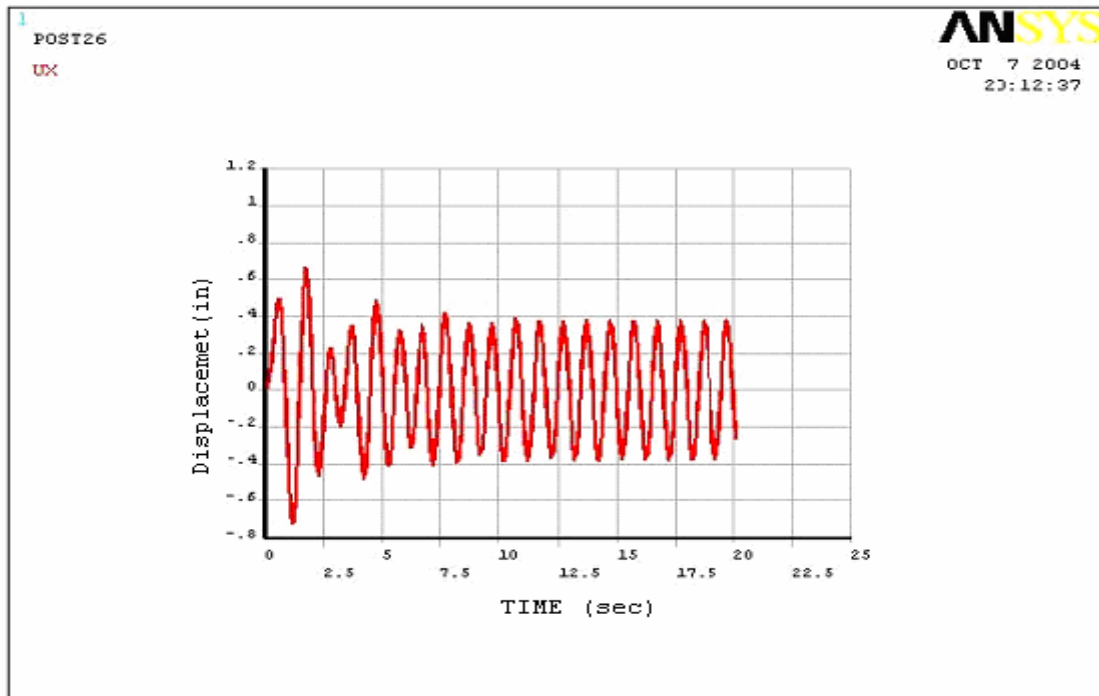
Figure 5.14: Axial response of the mass with damping by applied using force calculations

71

5.3.2CASE2: Flexible beam subjected to Lateral excitation

As a second case of verification, a transient response is simulated for a flexible cantilever beam by subjecting one end of the beam to a lateral harmonic load. In this case, at first, damping is included in the transient analysis by using Combin 14 elements along the beam. If we assume zero stiffness for the Combin14 elements, the spring–damper element becomes simply a dashpot. Again, for comparison, the same transient analysis is performed by including velocity-proportional damping by calculating damping forces as described in section 5.2. But in this case, the damping force is proportional to velocity, but not the square of the velocity. The free end lateral response obtained with application of damping by force calculations is compared with the response obtained with inclusion of damping by the Combin14 element, to verify the quadratic damping implementation in ANSYS for nonlinear transient simulations of the flexible cantilever beam. The dimensions and material properties are given in Chapter4, Section 4.2. Figure 5.15 shows a schematic diagram of the beam subjected to a transverse harmonic load with dampers at each node.
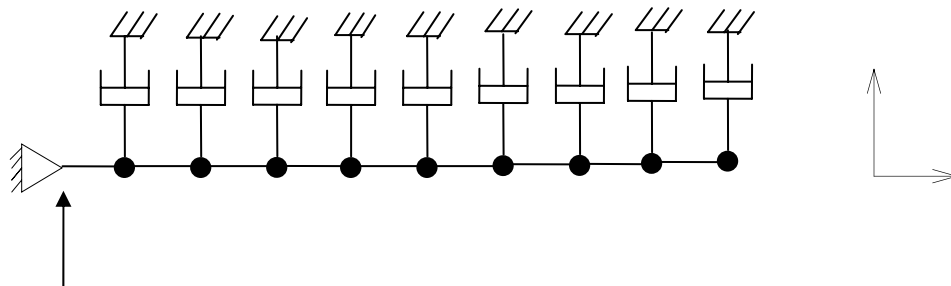
Figure 5.15: Flexible cantilever beam with damper at each node

The beam is subjected to harmonic load with an excitation frequency of 1 Hz, and the damping coefficient assumed for the analysis 0.00122, corresponding to a damping ratio of 0.1. Beam3 element of ANSYS is used to model the beam. The full method transient analysis option is used to simulate the transient response at the free end of the beam. At the location where harmonic load is applied laterally, the beam is constrained in the axial direction and in rotation about the z-axis. Geometric nonlinearities and gravity effects are included in the simulations. Figure 5.16 shows the lateral free end response obtained by including damping with Combin14 elements (dashpots). Figure 5.17 shows the lateral free end response obtained with application of damping by force calculations.
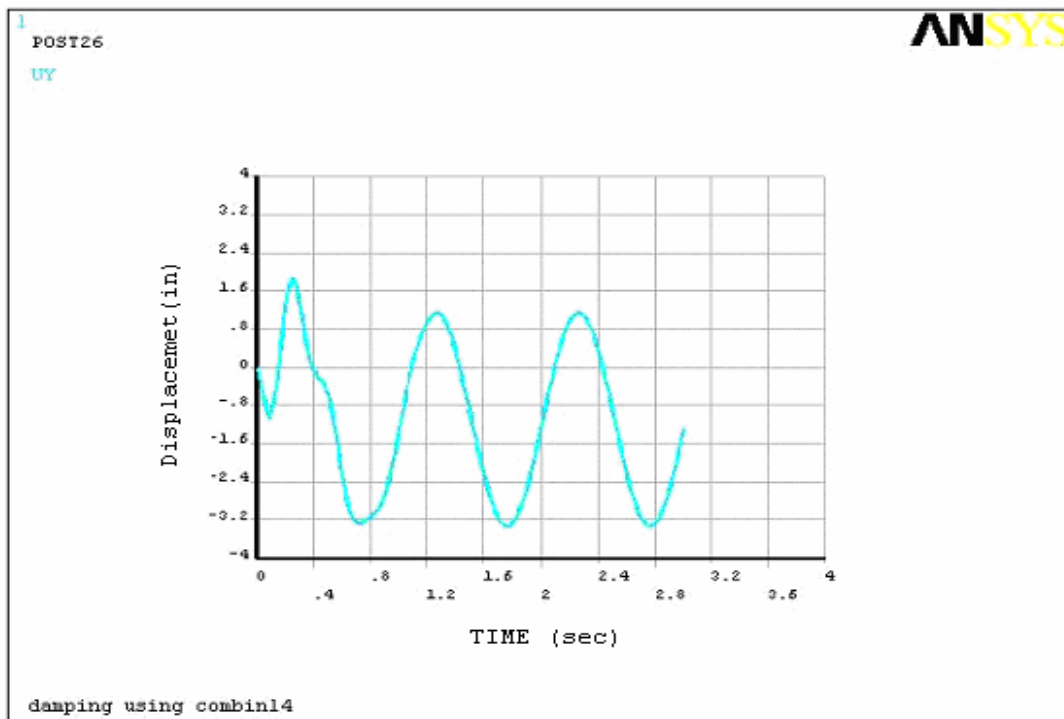
Figure 5.16: Lateral free end response by including damping with Combin14 elements
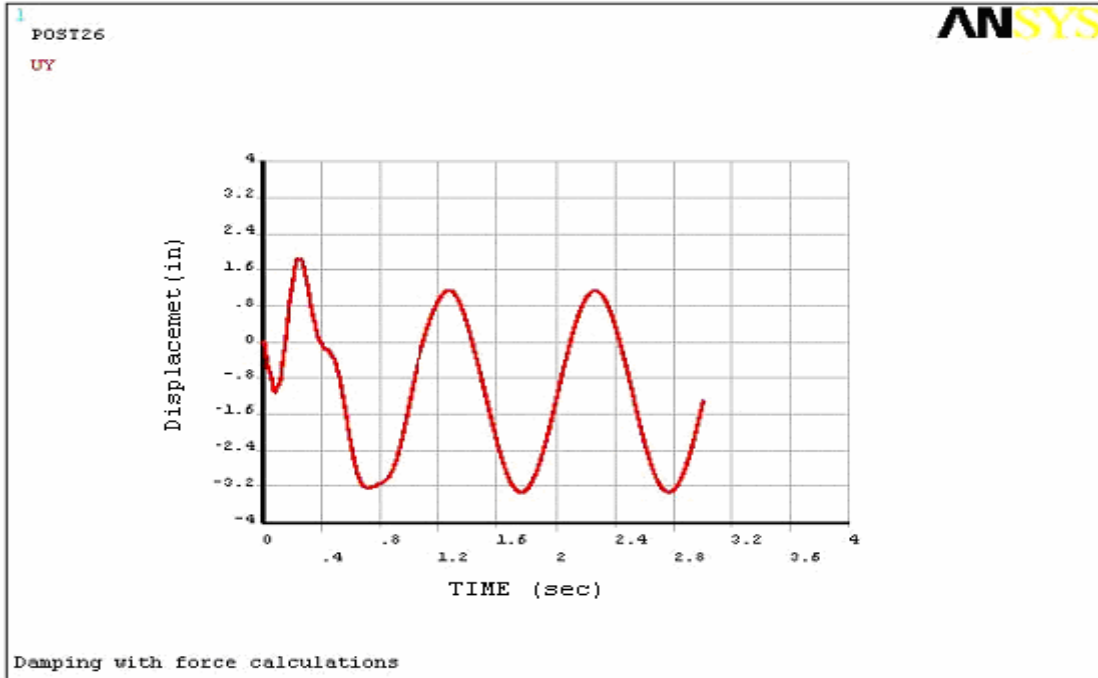
Figure 5.17: Lateral free end response by including damping with force calculations

Comparison of the lateral free end response in the figure 5.17 with the lateral free end response in Figure 5.16 verifies that the response obtained with both damping methods are in agreement.

Therefore, from the cases of axial response due to axial input, and lateral response due to lateral excitations, we can conclude that the results generated by damping force calculations are accurate. Hence, the method used to implement nonlinear transient simulation generated with quadratic damping is likely a reasonable approach

5.4 Effect of Damping Coefficient on Steady-State Response

 Nonlinear transient analysis is performed on the flexible cantilever beam with quadratic damping coefficients $50\times10^{-7}, 25\times10^{-7}$, 75×10^{-8}, and 25×10^{-8}, for the axial base excitation frequencies 1.21 Hz, 1.23 Hz,1.25 Hz, 1.27 Hz, 1.29 Hz, 1.31Hz and 1.33 Hz for 150 seconds. The flexible cantilever beam is modeled with 60 nodes, and the analysis is performed with a time interval of 0.001 seconds. Each nonlinear transient analysis takes approximately 25 hours of clock time.

In Figure 5.18, the lateral steady-state amplitude as function of excitation frequency is shown, for a range of damping coefficients over a range of excitation frequencies. The range of frequencies shown does not include 1.21 Hz and 1.33 Hz, because at these frequencies, there was no parametric response, only a decaying oscillation due to the lateral initial velocity that was assumed.

Figure 5.18 shows the expected result that steady-state amplitudes increase with decreasing assumed damping coefficient. Also, the largest steady-state amplitudes occur at frequencies in the selected range that are nearest 2X the first mode natural frequency.
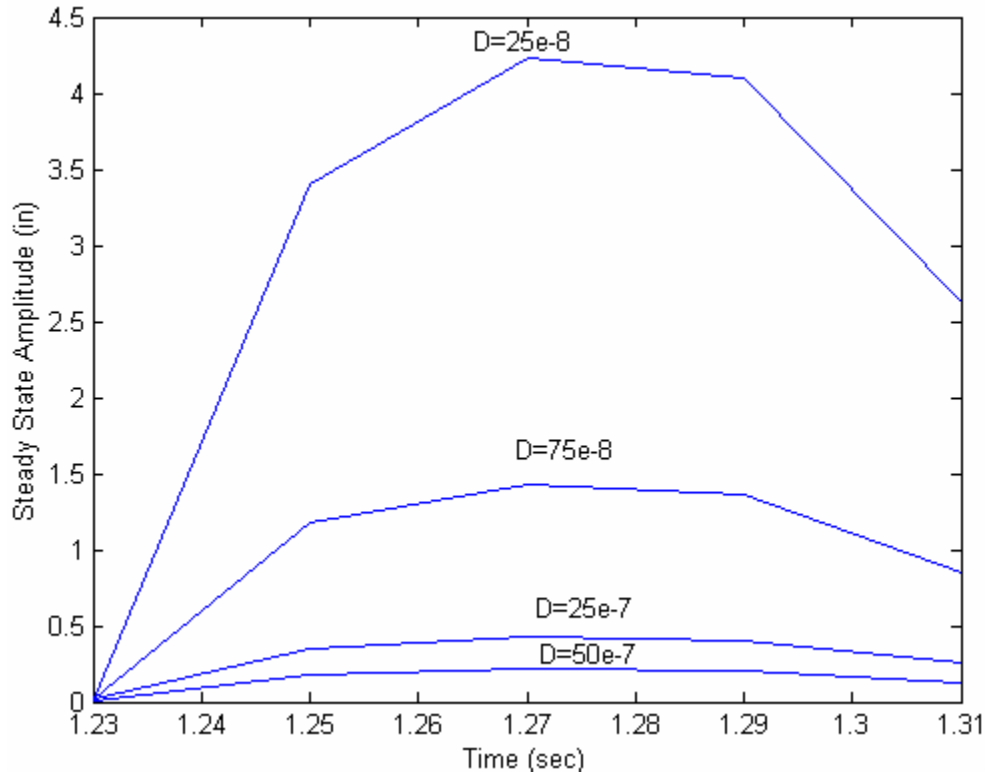
Figure 5.18: Steady-State Amplitude vs. Excitation Frequency

5.5 Observations on Response Phase with Respect to Input

The steady-state response for an excitation frequency *f=1.25 Hz* is considered here to explain a procedure developed in this work for defining and calculating a "response phase" with respect to the axial base excitation for the flexible cantilever beam. The phase in this case is different than the phase as usually defined in a linear harmonic response analysis. In a linear case, the input frequency and response frequency are identical. In these particular nonlinear parametric response cases, the input frequency is 2X the response frequency. It is not clear that there is any accepted definition of a "response phase with respect to input" in such a case. But, it does seem that, due to the fact that the input frequency is an integer multiple of the response frequency, a phase

angle can be defined, and perhaps study of this phase angle can lead to a better understanding of this nonlinear parametric response phenomenon.
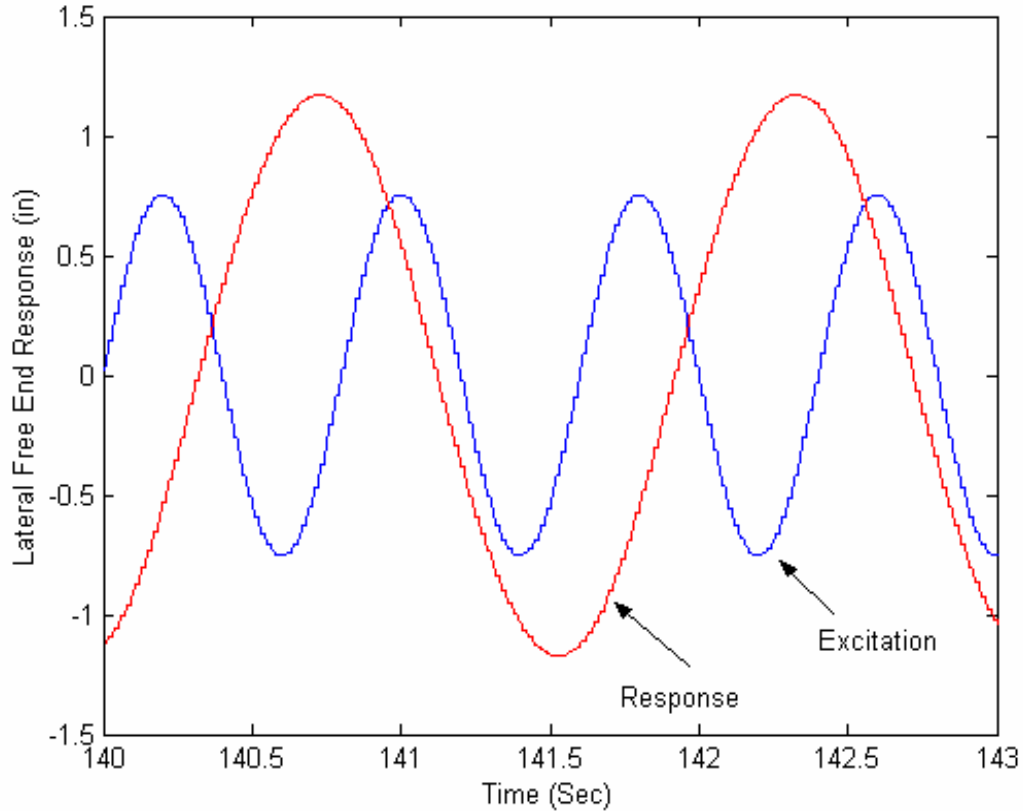
Figure5.19: Lateral free end response and axial base excitation with *f=1.25 Hz*.

Let $x(t)$ and $y(t)$ harmonic functions represent axial base excitation and lateral free end response, respectively, for the response shown in the figure 5.19. Equation 5.4.1 and 5.4.2 represents corresponding steady-state response and excitation functions for the case of an excitation frequency *f=1.25Hz:*

$$x(t) = 0.7542\sin(2w_r t) \tag{5.4.1}$$

$$y(t) = 1.1719\sin(w_r t - \phi) \tag{5.4.2}$$

Where

w_r = Frequency of the response

ϕ = "Phase Angle"

$$w_r = 2\pi f_r \tag{5.4.3}$$

$$f_r = \frac{1}{T_r} \tag{5.4.4}$$

Where

T_r = Time period for the response

 For this case, the response frequency can be calculated from the corresponding time
period, which is 1.59 sec. Let t_{py} be the time at which a peak occurs in the lateral
response function, and let t_{px} be the time corresponding to the most recent previous peak
in the excitation function. Then, Δt is given by the equation

$$\Delta t = t_{py} - t_{px} \tag{5.4.5}$$

Now, the phase difference, as defined here, can be calculated by using the equation
(5.4.8) obtained from equation (5.4.7)

$$\phi = \frac{1}{2}\left[2\pi \left(\frac{\Delta t}{T_r} \right) \right] \tag{5.4.7}$$

$$\phi = \pi(\Delta t) f_r \tag{5.4.8}$$

For this case, t_{py} and t_{px}, are 140.73 sec and 14.20 sec, and corresponding phase
difference calculated from equation (5.4.8) is 60 degrees, or 1.0471 radians.

The phase difference values are calculated for lateral steady-state response with respect to a range of axial base excitation frequencies, with four quadratic damping coefficients. Table5.1, Table5.2, Table5.3, and Table 5.4 present response phase results for damping coefficients of $D = 25 \times 10^{-8}$, 75×10^{-8}, 25×10^{-7}, and 50×10^{-7}.

The results show that for a given assumed damping coefficient value, D, increasing the excitation frequency in the range of the parametric response increases the corresponding response phase angle. Near the upper end of the parametric response region, it appears that for these cases, the phase angle, as defined in this work, approaches 90 degrees. Figure 5.20 shows a plot between base excitation frequency and response phase difference for quadratic damping coefficients $D = 25 \times 10^{-8}$, 75×10^{-8}, 25×10^{-7}, and 50×10^{-7}.

Table5.1: Response phase values for quadratic damping coefficient $D = 25 \times 10^{-8}$

Excitation Frequency Hz	Response Phase Degrees(Radians)
1.23	46.7243(0.8154)
1.25	58.3128(1.0177)
1.27	65.9808(1.1518)
1.29	73.1430(1.2765)
1.31	81.6987(1.4259)

Table5.2: Response phase values for quadratic damping coefficient D=75×10^{-8}

Excitation Frequency Hz	Response Phase Degrees(Radians)
1.23	47.7777(0.8333)
1.25	60.0000(1.0471)
1.27	68.9060(1.2026)
1.29	74.8000(1.3055)
1.31	82.8900(1.4467)

Table5.3: Response phase values for quadratic damping coefficient D=25×10^{-7}

Excitation Frequency Hz	Response Phase Degrees(Radians)
1.23	47.777(0.8338)
1.25	59.2546(1.0146)
1.27	66.0759(1.1532)
1.29	74.8000(1.3055)
1.31	80.0004(1.3400)

Table5.4: Response phase values for quadratic damping coefficient D=50×10^{-7}

Excitation Frequency Hz	Response Phase Degrees(Radians)
1.23	47.3535(0.8264)
1.25	59.6250(1.0406)
1.27	67.6430(1.18059)
1.29	73.8400(1.2888)
1.31	82.8900(1.4467)
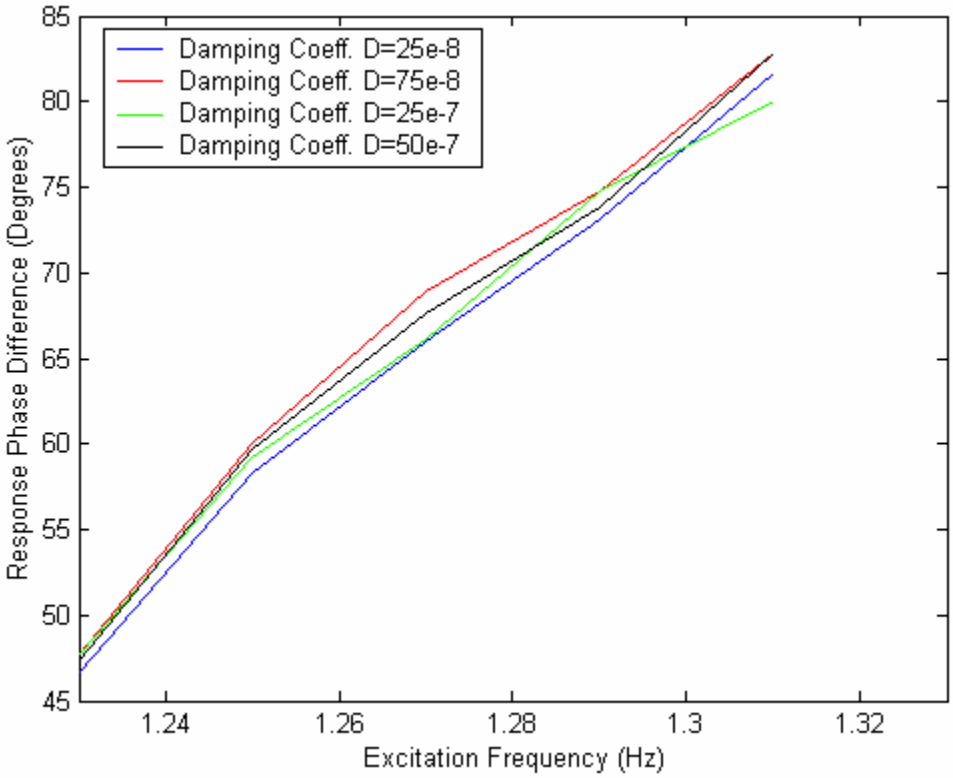
Figure5.20: Excitation frequency Vs Phase Difference for quadratic damping coefficients 25e-8, 75e-8, 25e-7, 50e-7

CHAPTER 6
SUMMARY, CONCLUSIONS, AND FUTURE WORK

6.1 Summary and Conclusions

The primary focus of this work was the development and implementation of procedures for performing transient analysis of nonlinear parametric response of a flexible cantilever beam assuming axial base excitation and quadratic damping using the commercial finite element code, ANSYS. The procedures were developed, and to illustrate their use, simulations were performed to calculate parametric response of a flexible beam, where the response was in the beam's first mode. ANSYS does have a preprogrammed method to implement quadratic damping using combin14 elements. But, a different, more flexible approach for quadratic damping was successfully implemented in this work and included in the analysis of the beam.

The implemented procedure for quadratic damping in ANSYS was confirmed by considering the case of velocity-proportional damping, and comparing results from application of damping by force calculations with results from application of damping by using Combin14 elements (dashpots) for two cases. The two cases considered were the lateral response of a beam due to lateral excitation, and the response of single degree freedom spring–mass system due to axial support excitation. The comparison showed essentially identical results for both confirmation cases. The quadratic damping

procedure that was developed was applied in a study of the variation of the steady-state amplitude of beam parametric response for a range of quadratic damping coefficients, over a range of excitation frequencies.

An additional contribution of this work was the definition and calculation of a "phase angle" for the nonlinear parametric response case. The response phase with respect to input was studied for a range of excitation frequencies and a range of damping coefficients. For the cases considered in this work, the response phase, as defined in this work, increases with increasing excitation frequency within the range of excitation frequencies in which parametric response is predicted. Further, it appears that, for the cases considered, at the upper end of the excitation frequency range in which parametric response is predicted, this response phase approaches 90 degrees. There does not appear to be a dependence of phase angle on quadratic damping coefficients, D.

In addition, the implicit finite element and explicit dynamic finite element methods were compared for the beam's lateral response due to lateral excitations, and for the beam's lateral response due to axial parametric excitation. Both the methods generated stable and accurate results for the beam's lateral response due to lateral excitations. For the case of parametric response of the beam due to axial base excitation, the implicit finite element method generated the expected, steady-state response with constant amplitude. But, for the modeling parameters assumed in this work, the explicit method produced results that, at least in some cases, did not have clear constant steady-state response amplitude.

6.2 Future Work

In this thesis, a method for implementing quadratic damping in the analysis of parametric response of flexible beams due to axial excitation was successfully developed. Also, a definition of response phase with respect to input was developed. Initial studies regarding effect of quadratic damping on response and the effect of excitation frequency on phase angle were completed. This work could be used as a basis for a wide range of studies in the important field of nonlinear dynamic systems analysis. A few suggestions for further studies building on this work are outlined below:

1. The quadratic damping approach could be applied to study the conditions under which this type of damping (related to fluid forces) is significant as compared to the more standard assumption of structural velocity-proportional damping.

2. The quadratic damping approach could be applied to study behavior of structures of perhaps more practical importance, such as cable stayed-bridge cables.

3. The response phase over a wider range of excitation frequencies and damping coefficient values could be calculated, and the results may provide further insights into the parametric response phenomenon. This phase angle calculation approach can be applied to cases with alternative damping assumptions. It could also be applied to cases where higher modes are excited parametrically.

4. The analysis procedures could be further refined to be made more efficient in terms of solution time.

Appendix A

MATLAB m-file to Generate Newmark's Numerical Integration Solution

```
function [u,a,v]=nm(i)
m=2;
c=4;
k=18;
f=1;
alpha=0.25;
delta=0.5;
dt=0.1 ;
A0=1/(alpha*dt^2);
A1=delta/(alpha*dt);
A2=1/(alpha*dt);
A3=(1/(2*alpha))-1;
A4=(delta/alpha)-1;
A5=(dt/2)*((delta/alpha)-2);
A6=dt*(1-delta);
A7=delta*dt;
u(1)=0;
v(1)=0;
a(1)=0;
n=70
for i=1:n,
u(i+1)=(f+m*(A0*u(i)+A2*v(i)+A3*a(i))+c*(A1*u(i)+A4*v(i)+A5*a(i)))/(A0*m+A1*c
+k);
a(i+1)=(A0*(u(i+1)-u(i)))-A2*(v(i))-A3*(a(i));
v(i+1)=v(i)+A6*a(i)+A7*a(i+1);
end
t=0:0.1:7;
plot(t,u)
```

Appendix B

MATLAB m-file to Generate Newmark's Numerical Integration Solution

```
function [u,v,t]=centraldiff
m=2;
c=4;
k=18;
j=70;
r=0.1;
u(1)=0;
v(1)=0;
beta=1/(2+(0.6*r)+(3*(r^2)));
a=beta*r;
u(2)=(a*(r^2))/6;
v(2)=(a*r)/2;
t(1)=0;
t(2)=r;
fa=1;
for i=2:j,
   t(i+1)=i*j;
   u(i+1)=2*u(i)-u(i-1)-((r^2)*k/m)*u(i)-((r^2)*c/m)*v(i)+(r^2/m)*fa;
   v(i+1)=(1/r)*(u(i+1)-u(i))+((r/m)*(-k*u(i)-c*v(i)+fa));
end
t=0:0.1:7;
plot(t,u,'r')
```

Appendix C

ANSYS – Batch file for simulating nonlinear response of a cantilever beam including Quadratic Damping

```
/filnam,d25em7f1p27
/config,nres,100001
/prep7
/title,Damping with force calculations
/nerr,999999,999999
f=1.27                                          ! Axial Base Excitation Frequency
a=46.53/((2*3.14159265359*f)**2)
et,1,3
r,1,.75*.032,(1/12)*.75*(.032**3),.032,6/5
ex,1,30e6
nuxy,1,.29
dens,1,.00073
type,1
real,1
mat,1
numnode=60                                      ! Number of nodes
dt=0.001                                        ! Initial Time Step
d=0.0000025                                     ! Damping Coefficient
n,1
n,numnode,33.56
fill
e,1,2
*repeat,numnode-1,1,1
*dim,disp,table,100001
*dim,uyold,array,numnode
*dim,uxold,array,numnode
*dim,frcy,array,numnode
*dim,frcx,array,numnode
*do,i,1,100001
        t=(i-1)/1000
        disp(i,1)=a*sin(2*3.14159265359*f*t)    ! Axial base displacement function
        disp(i,0)=t
*enddo
d,1,uy,0
d,1,rotz,0
d,1,ux,%disp%
/solu
```

```
RESCONTROL,DEFINE,NONE,NONE                    ! Activating Single Frame Restart
antype,trans
trnopt,full
nlgeom,on                                      !Geometric Nonlinearities
sstif,on
acel,386.5
alphad,0.00001
ic,numnode,uy,,0.5                             ! Initial Transverse Velocity
nsel,s,node,,1
nsel,a,node,,numnode
cm,resnodes,node
allsel
outres,all,none
outres,nsol,last,resnodes
deltim,dt,dt,dt
time,dt
solve
save
finish
```

!velocity-squared damping force calculations for initial time interval

```
/post1
*do,j,2,numnode
        uyold(j)=0
        uxold(j)=0
        *get,uynew,node,j,u,y
        *get,uxnew,node,j,u,x
        vely=(uynew-uyold(j))/dt
        velx=(uxnew-uxold(j))/dt
        uyold(j)=uynew
        uxold(j)=uxnew
        *get,phi,node,j,rot,z
        vnorm=(vely*cos(phi))-(velx*sin(phi))
        fnorm=-d*vnorm*abs(vnorm)                          ! Velocity  Squared  Damping
Calculation
        frcx(j)=-fnorm*sin(phi)
        frcy(j)=fnorm*cos(phi)
*enddo

*do,i,1,100000
         /solu
        RESCONTROL,DEFINE,NONE,NONE    ! Activating Single Frame Restart
        antype,trans,rest                          ! Restarting Transient Analysis
        fdel,all
        *do,k,2,numnode-1
```

```
            f,k,fy,frcy(k)                          ! Application of velocity –squared
       damping
            f,k,fx,frcx(k)
        *enddo
        f,numnode,fy,frcy(numnode)/2
        f,numnode,fx,frcx(numnode)/2
        time,(i+1)*dt
       solve
       finish
       /post1
       *do,j,2,numnode
            *get,uynew,node,j,u,y
             *get,uxnew,node,j,u,x
            vely=(uynew-uyold(j))/dt
            velx=(uxnew-uxold(j))/dt
            uyold(j)=uynew
            uxold(j)=uxnew
            *get,phi,node,j,rot,z
            vnorm=(vely*cos(phi))-(velx*sin(phi))
            fnorm=-d*vnorm*abs(vnorm)
            frcx(j)=-fnorm*sin(phi)
            frcy(j)=fnorm*cos(phi)
        *enddo
*enddo
save

finish
/post26
lines,1000000
/output,d25em7f1p27res,txt
nsol,2,1,u,x,n1ux
nsol,3,numnode,u,y,n60uy
prvar,2,3
/output
timerang,90,100
/output,d25em7f1p27last,txt
prvar,2,3
/output
fini
/eof
```

Appendix D

ANSYS – Batch file for simulating lateral response of the beam for lateral input including Damping by Combin14

```
/filname, dampcombin14
/config,nres,5000
/title, damping using combin14
/prep7
/nerr,999999,999999
et,1,3
n,1
n,10,33.56
fill
r,1,.75*.128,(1/12)*.75*(.128**3),.128,6/5
ex,1,30e6
nuxy,1,.29
dens,1,.00073
type,1
real,1
mat,1
e,1,2
*repeat,9,1,1
et,2,combin14
r,2,,0.00122                                ! Applying damping  by Combin14 element
n,11,3.72,1
n,19,33.56,1
fill
type,2
real,2
*do,i,2,10,1
        e,i,i+9
        d,i+9,all
*enddo
type,2
real,3
e,10,40
d,40,all
*dim,disp,table,1001
*do,i,1,1001
        t=(i-1)/100
```

```
        disp(i,1)=2*sin(2*3.14159*1*t)
        disp(i,0)=t
*enddo
d,1,ux,0
d,1,rotz,0
d,1,uy,%disp%
/solu
antype,trans
trnopt,full
nlgeom,on
sstif,on
acel,,386.4
deltim,0.01
time,3
autots,on
outres,all,all
solve
save
finish
```

Appendix E

MATLAB m-file to calculate Response phase with respect to input

```
f=1.28                          % Excitation frequency - input for running program
[time,ux,uy]=textread('40node.m','%f %f %f ','headerlines',3);
plot(time,uy)                   % Transient Response of free end of cantilever Beam
hold on;
plot(time,ux,'r')               % Axial Base Excitation of cantilever Beam
p=[time  uy];
k=1;
l=1;
% Searching for Time values where deflection is maximum both in Excitation
% and Response
for i=1:10000
        j=i;
        u1=uy(i);
        u2=uy(i+1);
        u3=uy(i+2);
        if (((u2>=u1)&(u2>u3)))
                j=i+1;
                peak=u2;
                pq(k)=time(j);            %Time values for peaks in Response
                k=k+1;
        end
y1=ux(i);
y2=ux(i+1);
y3=ux(i+2);
        if (((y2>=y1)&(y2>=y3)))
                j=i+1;
                peake=y2;
                yt(l)=time(j);            % Time values for peaks in excitation
                l=l+1;
        end
end
tpr=pq;
tpe=yt;
a=k-1;
b=2*a;
m=l-1;
n=1;
% Calculation of delta 't'(difference of peak times)
```

```
if (m==b)
        for i=1:a
        j=((2*i)-1);
                if (j<=m)
                delt(n)=tpr(i)-tpe(j);
                n=n+1;
                end
        end
end
if (m>b)
        for i=2:a
                j=2*i;
                if (j<=m)
                delt(n)=tpr(i)-tpe(j);
                n=n+1;
                end
        end
end
if (m<b)
for i=2:a
        j=((2*i)-2);
                if (j<=m)
                delt(n)=tpr(i)-tpe(j);
                n=n+1;
                end
        end
end
dt=abs(delt);
phase_diff=180*(dt)*f;                    %Calculation of Phase Difference
phase_diff_avg=sum(phase_diff)/(n-1)      %Calculation of Average Phase Difference
```

REFERENCES

1. ANSYS online Help. ANSYS Release 8.0 (2003) SAS IP, INC.

2. Hallquist, John O., LS-DYNA Theoretical Manual, Livermore Software Technology (1998)

3. Nayfeh, A.H. and Mook, D.T., Nonlinear Oscillations, John Wiley and Sons, New York, Inc (1979).

4. Mei, K., "Nonlinear Vibration of Beam Structures: Analytical and Explicit Dynamics FEA Evaluations". PhD Dissertation, University of Kentucky (2000).

5. Anderson, T.J., "Nonlinear Vibrations of Metallic and Composite structures". PhD Dissertation, Virginia Polytechnic Institute and State University (1993).

6. Cartmell, M., Introduction to Linear, Parametric and Nonlinear Vibrations, Chapman and Hall (1958).

7. Nayfeh, A.H and Mook D.T., Introduction to perturbation Techniques, John Wiley and Sons, New York, Inc (1977).

8. Crespo da Silva, M.R.M and Glynn, C.C., "Nonlinear Flexural-flexural torsional dynamics of inextensible beams-I. Equations of Motion", J. Structural mechanics, Vol6, No.4, PP. 437-448 (1978).

9. Crespo da Silva, M.R.M and C.C. Glynn, "Nonlinear Flexural-flexural torsional dynamics of inextensible beams-II. Equations of Motion", J. Structural mechanics, Vol6, No.4, PP. 449-461 (1978).

10. Nayfeh, A.H and Pai P.F., "Nonlinear, non planar parametric responses of an inextensible beam", International Journal of Non-Linear Mechanics, Vol.24, No.2 pp 139-158 (1989)

11. Nayfeh, A.H., Chin, C.-M., and Nayfeh, S.A, "Nonlinear normal modes of a cantilever beam", J. of Vibration and acoustics 117, 477-481 (1995).

12. Arafat, H.N., Nayfeh, A.H, and Chin, C, "Nonlinear non planar dynamics of parametrically excited cantilever beams", Nonlinear Dynamics, Vol. 1525, pp 31-61 (1998).

13. Hamdan, M.N., Al-Qaisia, and A.A, Al-Bedoor, B.O., "comparison of analytical techniques for nonlinear vibrations of a parametrically excited cantilever beam", J. of Mechanical Sciences, Vol. 43, No.6, pp 1521-1542 (2001).

14. Nayfeh, A.H, Yabuno, H., "Nonlinear modes of a parametrically excited cantilever beam. Nonlinear Dynamics", Vol. 25, pp 65-77 (2001)

15. Anderson, T.J., Nayfeh, A.H, and Balachandran, B., "Experimental verification of the importance of the nonlinear curvature in the response of a cantilever beam", J. of Vibration and acoustics, Vol. 118, pp 21-27 (1996).

16. Mei, K., Smith, S.W., Lovell, M.R., " Explicit dynamics finite element analysis for parametrically excited motion of a cantilever beam", Proceedings of the international Modal Analysis conference- IMAC, Vol.1, pp 733-739 (2000)

17. Hu, X., Wagoner, R.H., Daehn, G.S., Ghosh, S., "Comparison of explicit and implicit finite element methods in the quasistatic simulation of uniaxial tension", Communications in Numerical Methods In engineering, Vol. 10, 993-1003 (1994).

18. Rebelo, N., Nagtegaal, J.C. and Taylor L.M., "Comparison of implicit and explicit finite element methods in the simulation of metal forming processes", Numerical Methods in Industrial Forming Processes, PP 99-108 (1992)

19. Wang, S.P, Choudhry, S., Wertheimer, T.B., "Comparison between the static implicit and dynamic explicit methods for FEM simulation of sheet forming processes"

20. Sun, J.S., Lee, K.H., and Lee, H.P., " Comparison of implicit and explicit finite element methods for dynamic problems', J. of Materials processing Technology, Vol.105 , pp 110-118 (2000)

21. Implicit Versus Explicit methods, Flow science Inc, http://www.flow3d.com/

22. Bathe, K. J., Finite Element Procedures, Prentice-Hall, Englewood Cliffs, NJ. 1982

23. Cook, R. D., Malkus, D.S., and Plesha, M.E., Concepts and Applications of Finite Element Analysis, Second Edition, John Wiley and Sons, New York (1981).

24. Blevins, R.D., Applied Fluid Dynamics Hand Book, Krieger Publishing Company (1992).

25. Robert, A.N. and Olsson, M.G., "The Pendulum-Rich Physics from a simple system", Am. J. Physics, Vol. 54, No.2 (1986)

26. Jean, D.P. "Nonlinear finite Element Simulations of Large oscillations of Flexible Structures with Applications to Bridge Stay Cables", MS Thesis, University of Kentucky (2003).

27. Smith, S.W., Provided Image of Fred Hartman Bridge, Houston, TX.

28. International Space Station Image, NASA image gallery,
    http://observe.arc.nasa.gov/nasa/gallery/image_gallery/flight/flight_ISS2.html

29. Thomson, W.T. and Dahleh, M.D., Theory of vibration with Applications,
    Prentice Hall, (1997)

30. Zienkiewicz, O. C., The Finite Element Method, McGraw-Hill Company,
    London, (1977).

VITA

I was born in a small town Eluru, A.P, INDIA on August 19, 1978 and lived there for eighteen years until I moved to Guntur to attend RVR&JC college of Engineering for my bachelors in Industrial and Production Engineering. I received my Bachelors degree in June 2000. After two years, I came to the United States of America to attend the University of Kentucky in August 2002. I joined the Masters program at the University of Kentucky with Mechanical Engineering as my major.

Satish Remala